

國立臺灣大學醫學院微生物學研究所



博士論文

Graduate Institute of Microbiology

College of Medicine

National Taiwan University

Doctoral Dissertation

RhoA異型體2位點R176G上核糖核酸編輯致

體細胞突變促進肺腺癌腫瘤發展

Somatic RNA-edited RHOA isoform 2-R176G variant
promotes tumor progression in lung adenocarcinoma

陳冠儒

KUAN-JU CHEN

指導教授：周玉山 博士

Advisor: Yuh-Shan Jou, Ph.D.

中華民國 112 年 2 月

February 2023



致謝

長達八年多的博士班真的十分艱辛，一路走來幾乎每個轉折就覺得是盡頭，數度想放棄；但我似乎是個非常非常幸運的人，在我沮喪、茫然時總有親朋好友學長學姊或長輩們出現扶持我，讓我關關難過關關過。我想我身邊的每一位都是我的貴人，心裡充滿無限感激。

回想當時剛加入實驗室的時候，我的程度和能力並沒有辦法跟得上大家，很多時候挫折就像是一種習慣，總是出其不意出現在我的生活，那種無所適從甚至是消極自卑的滋味，真的是一言難盡。然而博士班就像是一場砥練心智及毅力的修練，就像周玉山老師說的“Never look down on yourself.”我並不想放棄，所以繼續咬牙撐了下去，才有今天的我。

感謝我的口試委員楊瑞彬老師、林文昌老師、葉秀慧老師以及陳小梨老師，給了我很多專業建議並且包容我的不足也提醒我許多新的方向。也感謝 N606 實驗室的夥伴們，謝謝德倫學長一家人對我的照顧，謝謝我的哥哥宗傑及嫂嫂貞尹女士每天督促我，謝謝彥荔和麗瑾對我人生方向上的提點，謝謝思碩的大力幫忙，謝謝欣怡學姐和婕妤對我的關愛，謝謝小明學長、育瑄、穎之、舒靖、佳儀以及 Anh Thu，謝謝靖翔和柔合在研究上對我的幫助且不厭其煩的教我，感謝每一位在中研院以及認識且照顧我的朋友。也要謝謝我的好朋友黃嘉郁、政彥和心偉陪我度過那些開心的日子，還有謝謝我的好友芝瑜及瑩妤的鼎力相助。

尤其我要感謝周玉山老師，老師是我一生的貴人，如果沒有老師，我沒有辦法順利投 Paper 也無法順利畢業。謝謝老師總是在我實驗遇到瓶頸時給我更多不同角

度的想法和支持，是人生的明燈。我對老師的感激之情難以言喻。



最後，謝謝我的家人:爸爸陳世英先生、媽媽張麗雀女士、以及妹妹陳冠群和陳冠鑫，對於讀了這麼多年博士班又每天看起來很廢的我給予無限包容和陪伴。

以上的每一位，都是我人生的貴人，因為有你們，我才有繼續前進的勇氣。



Chinese abstract

(A-to-I) 核糖核酸編輯事件是在轉錄組中最常見的轉錄後核糖核酸編輯修飾，腺苷 (Adenosine) 轉換肌苷 (Inosine) 會造成體細胞突變和蛋白質組學的多樣性，然而其致癌性依舊極少探究。我們透過分析全基因組體細胞包含肺腺癌組織和配對的鄰近正常組織轉錄組中的(A-to-I) 核糖核酸編輯事件，一共得到 26280 個 RNA 編輯事件且主要發生在非編碼以及 Alu 重複的區域。其中體細胞(A-to-I)編輯事件造成的變異體包括 AZIN1-S367G, RHOA-R176G, TUBGCP2-N211S and RBMXL1-I40M 皆會形成錯義突變，而 MDM2-UTR and PPIA-UTR 則發生在 3 端非轉譯區，這些 RNA 編輯事件都能在 RNA 編輯資料庫以及藉由收集肺腺癌組織透過 SEQUENOM MassARRAY® System 方式驗證。有趣的是，體細胞 A-to-I 核糖核酸編輯事件發生在 RHOA 上不僅會造成錯義突變且只發生在 RhoA 變異體 2 的 3 端上而不是在主要的 RhoA 變異體 1 上。進一步發現，有表現 RHOAiso2-R176G 比起表現 RHOAiso2 的肺腺癌病患轉錄組出現與調節異常的 RHOA 功能、細胞增生、細胞轉移以及臨床結果相關的基因提升。大量表現 RHOAiso2-R176G 在肺腺癌細胞株會透過增加 RHOA-GTP 的活性並增加下游 Rock1/2 的磷酸化來提升細胞的增生和轉移並且在異種移植實驗中增加腫瘤的生長和轉移。總體而言，當(A-to-I) RNA 編輯事件發生在 RHOAiso2-R176G 會造成錯意突變且透過活化 RHOA-GTP/p-ROCK1/2 路徑能促進腫瘤發展，且可能成為在肺腺癌治療上針對蛋白異構體治療

與診斷的標靶。



關鍵字：肺腺癌、核糖核酸編輯事件、RHOA-R176G、SEQUENOM
MassARRAY® System、Rock1/2



Abstract

Adenosine to Inosine (A-to-I) RNA editing, the most common posttranscriptional editing in transcriptomes, causes somatic mutations and proteomic diversity but rarely explored their tumorigenicity. We conducted genome-wide somatic A-to-I RNA editing analysis of paired adjacent normal and lung adenocarcinoma (LUAD) transcriptomes and identified 26,280 editing events with majority of them residing in the non-coding and Alu repeat regions. Somatic A-to-I edited variants including AZIN1-S367G, RHOA-R176G, TUBGCP2-N211S and RBMXL1-I40M harbored nonsynonymous mutations, and MDM2-UTR and PPIA-UTR at the 3' untranslated region were validated in databases and in SEQUENOM MassARRAY® System on newly collected LUAD tissues. Interestingly, somatic RHOA A-to-I RNA editing sites caused nonsynonymous mutations occurred mainly at the unique 3'-end RHOA isoform 2 RNA (RHOAiso2), but not RHOA major isoform 1. Upregulated genes of RHOAiso2-R176G-expressing LUAD patient transcriptomes, in compared with that of RHOAiso2, are associated with aberrant RHOA functions, proliferation, migration and clinical outcomes. Expression of RHOAiso2-R176G in LUAD cells potentiates RHOA-GTP activity to phosphorylate ROCK1/2 effectors and enhance cell proliferation and migration and increase tumor growth in xenograft and metastasis models. In summary, somatic A-to-I edited isoform 2 specific

RHOAiso2-R176G mutation activated RHOA-GTP/p-ROCK1/2 signaling to promote tumor progression could be an isoform specific theranostic target in LUAD therapy.



Key words:

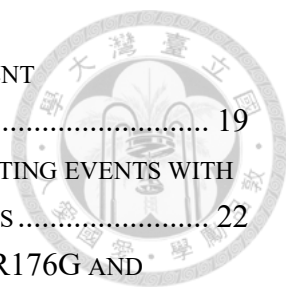
Lung adenocarcinoma, A-to-I RNA editing, RHOAiso2-R176G variant, SEQUENOM

MassARRAY® System, Rock1/2



Contents

致謝	I
CHINESE ABSTRACT	III
ABSTRACT	V
CONTENTS	VII
LIST OF FIGURES.....	IX
LIST OF TABLES.....	XI
CHAPTER1 INTRODUCTION.....	1
1.1 LUNG ADENOCARCINOMA	1
1.2 ADENOSINE-TO-INOSINE (A-TO-I) RNA EDITING.....	4
1.3 RAS HOMOLOG GENE FAMILY, MEMBER A, (RHOA).....	7
CHAPTER 2 MATERIALS AND METHODS	9
2.1 DATA SOURCES FOR IDENTIFY OF RNA EDITING EVENTS	9
2.2 GENE SET ENRICHMENT ANALYSIS	10
2.3 SEQUENOM MASSARRAY® SYSTEM	10
2.4 3D STRUCTURAL PREDICTION TO COMPARE RHOA ISOFORM 2 AND MUTANT PROTEINS	11
2.5 LUNG CANCER CELL LINES AND LUAD SAMPLES	12
2.6 SAMPLE PREPARATION AND CONSTRUCTS.....	12
2.5 FUNCTIONAL ASSAYS FOR LUAD CELL MIGRATION, TRACKING AND WOUND HEALING	13
2.6 RHOA-GTP PULL DOWN ASSAY.....	14
2.7 RT-PCR AND QUANTIFICATION OF RNA EXPRESSION	14
2.8 CELL PROLIFERATION ASSAYS	15
2.9 WESTERN BLOTTING ANALYSIS.....	15
2.10 TUMORIGENESIS IN ANIMALS	16
2.11 TAQMAN SYSTEM FOR DETECTION OF A-TO-I RNA EDITING EVENTS	16
2.12 EXPERIMENT OF CRISPR-CAS13 SYSTEM	17
2.13 KNOCKDOWN WITH shRNAs AND LENTIVIRAL INFECTIONS TO CELLS.....	18
CHAPTER 3 RESULTS	19



3.1 A-to-I RNA EDITING EVENTS WERE IDENTIFIED IN LUAD PATIENT TRANSCRIPTOMES	19
3.2 VALIDATION OF <i>IN SILICO</i> IDENTIFIED SOMATIC A-TO-I RNA EDITING EVENTS WITH SEQUENOM MASSARRAY® SYSTEM IN LUAD PATIENT SAMPLES	22
3.3 COMPARISON OF GENE SIGNATURES BETWEEN THE RHOA _{ISO2} -R176G AND RHOA _{ISO2} EXPRESSING LUAD PATIENT TRANSCRIPTOMES	27
3.4 EXPRESSION OF RHOA _{ISO2} -R176G INCREASED CELL PROLIFERATION AND MIGRATION IN LUAD CELLS.....	30
3.5 EXPRESSION OF RHOA _{ISO2} -R176G INCREASED TUMOR GROWTH AND METASTASIS	32
3.6 EXPRESSION OF RHOA _{ISO2} -R176G INCREASED RHOA-GTP ACTIVITY AND DOWNSTREAM PHOSPHORYLATED ROCK1/2 SIGNALING	33
CHAPTER 4 DISCUSSION AND CONCLUSION	35
REFERENCE	40

List of Figures



Figure 1 The schematic drawing of identifying A-to-I RNA editing events in LUAD transcriptomes with tumor and the corresponding normal pair.	45
Figure 2 The detail pipeline for identification of genome-wide A-to-I editing events of LUAD transcriptomes and validation in the known editing databases in silico.	46
Figure 3 RNA mismatch types.	47
Figure 4 Identify the region of informative editing sites.	48
Figure 5 The sample counts of RNA editing events in 23 LUAD patients.	49
Figure 6 SEQUENOM MassARRAY® System method to validate A-to-I RNA editing extents and editing ratio formula.	51
Figure 7 The RNA editing frequency of Selected A-to-I RNA editing sites in LUAD cell lines.	52
Figure 8 The RNA editing frequency of Selected A-to-I RNA editing sites in paired LUAD samples(n=20).	54
Figure 9 Expression of RHOA alternative splicing isoforms in normal (GTEx) and cancer (TCGA) tissues in UCSC Xena.	55
Figure 10 Nonsynonymous A-to-I RNA editing sites preferentially located at the unique C-terminal of RHOA isoform 2 but not the major isoform 1 of RHOA.	56
Figure 11 The schematic drawing of RhoA isoform 1 and 2 domains.	57
Figure 12 Expression of RHOA isoforms and RHOAiso2-R176G in LUAD cell lines by using TaqMan platforms.	58
Figure 13 ADAR1 expression modulates A-to-I RNA editing led to RHOAiso2-R176G mutation.	59
Figure 14 Comparison of predicted structures in between RHOAiso2 and RHOAiso2-R176G by using I-TASSER.	61
Figure 15 Comparison of gene signatures between the RHOAiso2-R176G and RHOAiso2 expressing LUAD patient transcriptomes.	63
Figure 16 The protein expression level of RhoAiso2 and RhoAiso2-R176G in LUAD cell lines.	64
Figure 17 Validation of enrichment gene signatures in the RHOAiso2-R176G mutation compared with RHOAiso2- expressing LUAD cell lines.	66
Figure 18 The distribution of present of RhoAiso2-R176G in 20 LUAD	

patients.....	68
Figure 19 RHOAiso2-R176G promoted cell proliferation and migration in LUAD cell lines compared to RHOAiso2.....	70
Figure 20 Expression of RHOAiso2-R176G mutation in LUAD cell line CL1-0.....	72
Figure 21 RHOAiso2-R176G variant promotes tumor growth and metastasis in vivo compared to RHOAiso2.....	74
Figure 22 RHOAiso2-R176G specific variant increased RHOA-GTP activity and phosphorylated p-ROCK1/2 signaling.....	76
Figure 23 Expression of RhoAiso2-R176G increased cell viability at RhoA inhibitor CCG-1423 treated.....	77



List of Tables

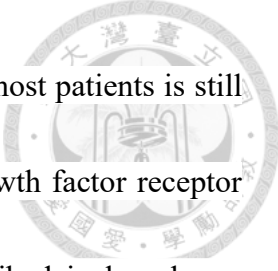
Table 1 A-to-I editing events in 20 paired LUAD	78
Table 2 Statistics.....	78
Table 3 Primer sequences of selected RNA editing sites for SEQUENOM MassARRAY® System.....	80
Table 4 Primer sequences for RT-qPCR of selected genes in functions of RHOA functions, cell proliferation, cell migration and clinical outcomes.	81
Table 5 Primer sequences for cloning and construction of RHOAiso2 and RHOAiso2-R176G site mutagenesis.....	83



Chapter1 introduction

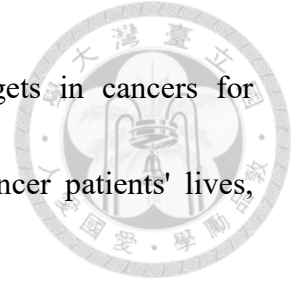
1.1 Lung adenocarcinoma

Lung cancer is the second most commonly diagnosed cancer among all genderin and as well as the leading cause of cancer death in Taiwan and around the world, with overall survival rate of 12% in 2022[1]. Depending on the stages, the overall survival rate from that stage1 70-85% to distant metastases is less than 5%[2]. The majority of newly diagnosed patients present with late stage metastatic lung cancer that are inoperable and resistant to therapies. Pathologically, lung cancers were divided into two major subtypes: non-small cell lung cancer (NSCLC) and small cell lung cancer (SCLC), comprised approximately 85% and 15% of patients, respectively[3]. Lung adenocarcinoma is the most common primary lung cancer seen in the United States. The main factor of risk is highly associated with smoking tobacco. Although the proportion of smoking people has declined, lung cancer is still widespread globally. Currently, the treatment of lung adenocarcinoma was based on the stage. Surgery is the better choice for early stage, but therapies for the advance stage patients including radiation therapy, chemotherapy, immunotherapy, target therapy and combined therapy are need. Because most diagnosed lung adenocarcinoma patients are incurable and advanced,



chemotherapy and target therapy are often used, but the survival of most patients is still dreadful. A subset of NSCLC is having mutations in epidermal growth factor receptor (EGFR) and anaplastic lymphoma kinase (ALK) which was described in lymphoma originally, but most ALK-positive cancers are in non-small cell lung cancer[4-6]. As therapeutic targets, EGFR mutation might have been treated with tyrosine kinase inhibitors, and ALK treated with ALK inhibitors as first-line target therapy. If the tumor is EGFR and ALK-negative, first-line chemotherapy is usually a platinum-based doublet, with bevacizumab as a possible third agent. KRAS mutation is the most frequent oncogene in non-small cell lung cancer around 20~40% of lung adenocarcinoma. In previous studies, KRAS mutant, a genetic biomarker for immune checkpoint inhibition, NSCLC are recommended for receiving chemotherapy and combined immunotherapy. When advanced NSCLC cannot be treated with targeted therapy, immunotherapy or immunotherapy combined with chemotherapy is often used. There are many FDA approves immunotherapy drugs to block PD-1 and PD-L1 pathway to treat NSCLC, including Atezolizumab, Durvalumab, Nivolumab and Pembrolizumab. FDA also approved Ipilimumab to block CTLA-4 pathway in combined with nivolumab to block PD-1 pathway or with chemotherapy [7-9]. Although treatments with inhibitors of molecular targets and immune checkpoints change the therapeutic paradigms with estimated increasing response rates and therapeutic benefit of ~30% of cancer patients

depending on cancer types, discover novel biomarkers and targets in cancers for developing innovative therapies remains critical to prolonging cancer patients' lives, including LUAD[10-12].





1.2 Adenosine-to-inosine (A-to-I) RNA editing

RNA editing is a common post-transcriptional modification event on selected RNA transcripts, which might be through two main enzymatic mechanisms: ADAR (Adenosine Deaminase that Act on RNA) family and APOBEC[13]. ADAR family converts Adenosine to Inosine and APOBEC can catalyze cytidine to uracil (C>U), but C>U is less common than A>I editing. A to G is the most common type of mismatch types. The ADARs family has three members ADAR1, ADAR2, and ADAR3. Comparing the Structures, ADAR2 has similar enzymatic domains with ADAR1.

ADAR3 has only been detected in brain and as an inhibitor of editing activity even though ADAR3 has enzymatic domains. [14]. In previous studies, Alu elements are the main targets of ADAR, because Alu elements can form a double strain RNA structure by repetitive reverse sequence. Alu elements are the most abundant repetitive elements and are interspersed throughout the human genome which might play an important role in editing of human transcriptome. According to editing events, it may increase transcriptome diversity via changes of the protein coding, RNA splicing and miRNA targets contributed to developmental complexity, and disease formation[15-18]. Moreover, there are more and more studies showing that RNA-editing events might play an important role in cancer progression. Although RNA-editing events are important to



cancer, there is still lack of detailed discoveries in LUAD.

Currently, based on modulate features and RNA editing activity of ADAR family, ADARs become biological tools not only for RBP target identification but also for therapeutic ADAR-based recoding. To date, CRISPR (Clustered Regularly Interspaced Short Palindromic Repeats) system has become a fixture in the laboratory and companies, CRISPR-Cas system is a therapeutic biology technique that can provide target DNA binding, cutting, editing, and integration. But CRISPR-Cas editing still has limitations. In previous researches, Cas9 which is one of enzyme used in CRISPR editing system could induce immune response and random Off-target effects to create unexpected mutations that influence on genome. Somehow, ADAR RNA editing could provide opportunities for RNA therapeutic in CRISPR system and allow clinicians to make temporary fixes to eliminate mutations in proteins, halt their production or change the way that they work in specific organs and tissue. However, RNA editing development is still far from perfect due to the characteristics of ADARs that could only change A-to-I RNA editing, therefore ADAR-CRISPR is relatively inefficient in modified plants and animals. [19-22].

Recently, there are three RNA editing databases including DARNED[23], REDportal[24] and The Cancer Editome Atlas (TCEA)[25]. In REDportal V2.0, RNA editing sites were collected from transcriptomes of human and non-human organisms with normal tissues in the Genotype-Tissue Expression (GTEx). The Cancer Editome Atlas (TCEA) RNA

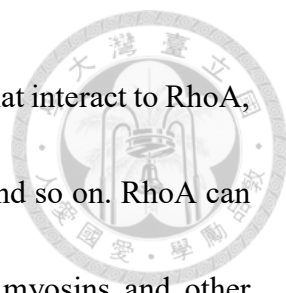
editing events were collected from 11,051 samples across 33 cancer types in The Cancer Genome Atlas (TCGA) projects. However, the functional and pathological impacts of the majority of A-to-I editing events during development and diseases are commonly neglected and underexplored.





1.3 Ras homolog gene family, member A, (RhoA)

The Ras homolog gene family, member A, (RhoA) is a small GTPase in the Rho family, and is involved in multiple oncogenic processes, including regulating cytoskeleton dynamics, cell morphology and polarity, cell motility, vesicle trafficking, cell cycle progression, cell survival, cell growth, and differentiation [26-28]. The RhoA gene is located on chromosome 3 and has 6 splice variants. There are 20 Rho GTPases in humans that can be classified into subfamilies according to their structural homology and mode of regulation. From the functional and structural data demonstrated that RhoA is composed of effector binding domain, GTP or GDP binding domain, hypervariable domain and the C-terminal with CAAX motif. RhoA GTPases perform as molecular switches in the regulation of multiple cellular processes. RhoA cycles between an inactive (GDP-bound) and active (GTP-bound) state which was regulated by guanine nucleotide exchange factors (GEFs) to activate Rho GTPases and GTPase-activating proteins (GAPs) to inactivate Rho GTPases. The hypervariable region is the most diverse among the 6 variants, which regulate RhoA membrane association while undergo palmitoylation[29-31]. When the C-terminus of RhoA undergoes post-translationally modification by geranylgeranylation[31], the RhoA translocate from membrane to the nucleus which might regulate cell growth and cytoskeletal organization.



In previous studies, there are many protein have been demonstrated that interact to RhoA, including downstream target protein ROCK1, ROCK2, MYBPH and so on. RhoA can activate downstream ROCK1/2, and activated ROCK1/2 regulate myosins and other actin-binding proteins in response to Rho which increases cell migration[32, 33]. In previous studies, RhoA activates focal adhesion kinase (FAK) signaling which leads to its increased association with the p85 regulatory subunit of phosphatidylinositol-3-kinase (PI3K) and to concomitant activation of Akt pathway[34].

RhoA has been reported in a variety of cancers, including, Breast carcinoma, testicular cancer, oesophageal squamous cell carcinoma, and lung tumor. Moreover, RhoA/ROCK signal is also involved in other disease, including hypertension, and regulated central nervous system. Most research is regarding RhoA isoform 1, but not other variants. RhoA isoform 2 has similar functional domains but has a different C-terminus which is still worth exploring.



Chapter 2 Materials and Methods

2.1 Data sources for identify of RNA editing events

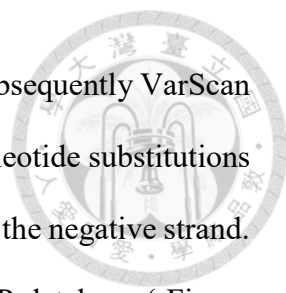
The transcriptome dataset of 23 lung adenocarcinoma patients were obtained from GSE40419 [35] at NCBI Gene Expression Omnibus (GEO).[36]. Human reference genome 19 (hg19) used in read alignment as reference genome were downloaded from UCSC Genome Browser. The transcriptomes in both normal and tumor tissues were collected and eliminated that derived from over 60 years old patients.

Read quality control was performed by Trimmomatic. Read base quality Q-score was set >30. First 14 bases of each read were cut due to inconsistent per base sequence content.[37, 38].

In normal condition, reads have an equal proportion of each nucleotides A, T, C, G about 25%, but there are large deviations from first 14 bp, to collect more precise data we trimmed first 14 bases of each read.

The range of quality base on position from the beginning to the end of the sequence. Typically with the illumina data, high quality sequence reads are from the beginning of the sequence down to about 3/4. Q-score was set >30. And trimmed the reads which quality below 25. We collected the reads only quality >30 and total obtained 87bp.

Read alignment was performed by STAR aligner[38]. Normal and tumor reads were aligned to the hg19 reference genome respectively. Novel splicing junctions were discovered during 1 pass mapping, and 2 pass mapping was performed to increase read coverage of regions that were downstream or upstream of splicing junctions. Alignments were sorted by chromosome coordinate. Duplicate reads were removed by Picard. We only kept uniquely mapped reads for analysis.



Normal and tumor alignments were processed with SAMtools and subsequently VarScan for the discovery of potential A to I editing sites, which were the nucleotide substitutions (gene to transcript) of A to G on positive reading strand and T to C on the negative strand. We eliminated the editing sites against known sites in NCBI dbSNP database (Figure 2)[39, 40].

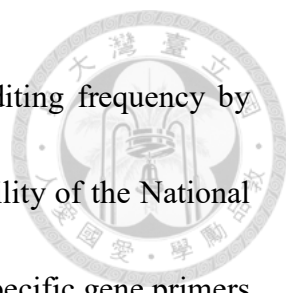
Filtered variants sorted as “Somatic” by VarScan were defined as cancer-specific A-to-I RNA editing sites. A list of candidates was created with 6 sets of editing sites of each patients. The list was intersected and annotated with known editing sites databases (RADAR[41] and DARNED[23]), candidate editing sites were annotated with the genomic locations with the gene name if available in ANNOVAR[42], repetitive region data (UCSC RepeatMasker[37]), and gene annotation data (GENCODE v19). The list of candidates was sorted by number of patients with the editing event.

2.2 Gene set enrichment analysis

For gene set enrichment analysis, we imported the differential expressed genes of LUAD transcriptomes into GSEA software (GSEA v4.2.3 for Windows) for analysis. We examined the enriched gene signatures including the hallmark and the curated gene sets and the ontology gene sets from the Molecular Signatures Database (MSigDB v7.4)[43].

2.3 SEQUENOM MassARRAY® System

AZIN1 (Chr.8: 103841636), MDM2 (Chr.12: 69237004), PPIA (Chr.7: 44842099), TUBGCP2 (Chr.10 135110893), RBMXL1 (Chr.1 89449390), and RHOA (Chr.3



49398382) candidate genes were selected to examine the RNA editing frequency by Sequenom MassARRAY (Sequenom Inc. CA, USA) at the core facility of the National Center for Genome Medicine in Academia Sinica of Taiwan. Two specific gene primers and one extension primer for each candidate target was designed by MassARRAY assay design software. The region (50-100bp) of candidate targets was amplified and the extension primer was hybridized editing sites. The non-edited and edited PCR product were generated and base on MALDI-TOF technology, two different PCR product were separated by different mass value (Tables 3 for all the sequences of primers) The RNA editing ratio is calculated based on the formula below.

Fold change of the RNA editing ratio=

$$\frac{G(cDNA)Height}{(A(cDNA) + G(cDNA))Height} / \frac{G(gDNA)Height}{(A(gDNA) + G(gDNA))Height}$$

2.4 3D structural prediction to compare RHOA isoform 2 and mutant proteins

We downloaded the RHOA isoform 2 (RHOAiso2 and C9JX21) sequences from the NCBI database and predicted the parental protein and its mutated peptide R176G by using the software I-TASSER[44, 45]. We selected the top models predicted by I-TASSER and chose the highest scores structures for further analysis.



2.5 Lung cancer cell lines and LUAD samples

Five LUAD cell lines including CL1-5, H1299, CL1-0, H23, A549 were maintained in DMEM medium with addition of 10% fetal calf serum, non-essential amino acid (Gibco, 11140), penicillin-streptomycin (Gibco, 15140), L-glutamine (Gibco, 25030081) in 5%CO₂ at 37°C incubator. After IRB approval No. (451)103A-28, we collected twenty paired tumor and adjacent normal tissue of LUAD patients from the Cheng Hsin General Hospital for validation experiments.

2.6 Sample preparation and constructs

Total RNA samples was extracted by TRIzol (Invitrogen) according to the manufacturer's instructions. RNA was reverse-transcribed into cDNA with oligo-dT primers using a Maxima H Minus First Strand cDNA Synthesis Kit (Thermo Scientific). Genomic DNA was extracted from 6 lung cancer cell lines and 20 Paired lung adenocarcinoma patients tumor and normal adjacent tissue from using DNeasy kit as per manufacturer's instructions (Qiagen). RHOA isoform 2 gene sequence was PCR amplified from immortalized cell line NL20cDNAs. The PCR product was subcloned into the expression vector pcDNA3-Flag. Site-directed mutagenesis was conducted to generate RHOAiso2-R176G form RhoAiso2. Tables 5 for the primer sequences.



2.5 Functional assays for LUAD cell migration, tracking and wound healing

In migration assay, migration assay, Cells (1×10^4 to 5×10^4) were added to the upper chamber of the $8 \mu\text{m}$ PET cell culture inserts (Millicell) and $700 \mu\text{L}$ medium containing 10% FBS was added into the lower chamber to incubate for 24 h.

Cells were then fixed with methyl alcohol for 30 min and stained with 0.5% crystal violet for 30 min. The stained cells on the filters were counted.

For wound healing assay, each well filed with $70 \mu\text{L}$ composed of cells (5×10^5 to 1×10^6 cells /ml) and medium into the insert and cultured in a 37°C incubator (ibidi culture-insert 2 well from the ibidi GmbH at Martinsried in Germany). After 17 to 24 hours for cell attachment, the culture-insert was removed and the well was refilled with fresh medium. Two automated photographs of wound healing fields was taken every 30 min (Model- Leica DMI 6000B) to capture at magnification of $20\times$ and analyzed with the MetaMorph image analysis software. All wound healing assays were repeated three times.

In the cell tracking assay, cells were seeded in low density in a 12-well plate and incubated in 37°C overnight. After cell attachment, migrated cells were photographed with the Model- Leica DMI 6000B microscope every 30 min for 24 hours and data was analyzed by using MetaMorph Image analysis software.



2.6 RHOA-GTP pull down assay

The LUAD cell lines (A549, CL1-0, and CL1-5) were transfected and overexpressed with RHOAiso2 and RHOAiso2-R176G and harvested after 30 mins treatment with or without Rho Activator I (Cytoskeleton, Inc Cat. # CN01). Based on the RHOA Activation Assay Kit from the Cell Biolabs Inc. (STA-403-A), we conducted experiments based on manufacturer's instruction with all procedures proceed on ice. Total cell lysate was evaluated by the Bradford assay kit. The agarose bead slurry of the Rhotekin RBD was incubated with 2 mg/ml of protein lysates with rotation at 4 °C for 1 hour. Then, the Rhotekin RBD Agarose bead slurry with removed supernatant was boiled with reduced 2X SDS-PAGE sample buffer followed by the Western blot assay.

2.7 RT-PCR and quantification of RNA expression

RT-PCR was carried out with SYBR Green PCR Master Mix (Thermo Scientific). For quantification of gene expression at RNA level, equal amounts of cDNA and primers were mixed with SYBR Green Master Mix (Thermo Fisher Scientific™) and performed PCR reaction in Applied Biosystems 7500 Real-Time PCR System. GAPDH served as the internal control for normalization. Tables 4 for the primer sequences of selected genes in RT-qPCR.



2.8 Cell proliferation assays

Cell proliferation assay was detected in triplicate wells by using PrestoBlue™ Cell Viability Reagent (Invitrogen™). A total of 1×10^3 CL1-5, CL1-0 or A549 cells were seeded per well in the 96-well plates. The cells were incubated in a 37 °C incubator. We analyzed the cell viability at days 0, 1, 2, 3, 4 and 5 after cell seeding by detecting the absorbance with a microplate reader.

2.9 Western blotting analysis

The total protein lysates were extracted from LUAD cells using RIPA lysis buffer containing additional protease inhibitor cocktail and phosphatase inhibitor (Roche). Protein concentration in the cell lysate was quantified by the Bradford assay kit. Lysates were loaded and separated in the 12% SDS–PAGE and then transferred to 0.2 μm PVDF membrane (Millipore). The PVDF blotting membrane was further probed with specific antibodies from 3 hours to overnight at 4 °C. The antibodies against specific proteins were listed and used for our Western blotting analysis: β-Actin (FNab00872, FineTest), Flag (F3165, Sigma), RHOA (#2117, Cell Signaling), p-Rock1 (phospho T455 + S456) (ab203273, abcam), p-Rock2 (Ser1366) (# PA5-34895, Invitrogen), Rock1/2 (ab45171, abcam). The PVDF membrane was then incubated with 1:10000 ratio HRP-conjugated

secondary antibodies for 1 hr at room temperature. The intensity of chemo-luminescence was detected by using the ImageQuant LAS 4000 mini.



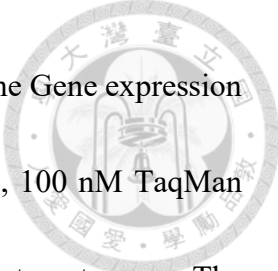
2.10 Tumorigenesis in animals

CL1-5 cells (3×10^6 in $100 \mu\text{l}$) transfectants of the RHOAiso2 wild type and RHOAiso2-R176G were mixed with Matrigel (BD Biosciences) at a 1:1 (v/v) ratio and subcutaneously injected into the opposite sites of the 8-week-old female BALB/c nude mice. Tumor volumes were measured and calculated as $(\text{width}^2 \times \text{length})/2$ and expressed in mm^3 . Tumors were resected and weighed after 4 weeks.

For systemic metastasis tail vein injection assay, mice were injected with CL1-5 transfectants (1×10^6) intravenously through tail vein. All mice were sacrificed after 4 weeks. The pulmonary tumor nodules were calculated after fixation of lungs with 10% formaldehyde for 48 h. All animal experiments were performed by following the guidelines and approved protocols from the institutional animal care and user committee.

2.11 TaqMan System for detection of A-to-I RNA editing events

The PCR primers and TaqMan probe specific for RhoAiso2 and GAPDH were designed using Realtime PCR Tool (Integrated DNA Technologies, inc.). We conducted the TaqMan real time quantitative PCR amplification reactions in the AB 7500 fast real-



time system. A 20 µl reaction mixture containing 10 µl IDT PrimeTime Gene expression Mater Mix, 400 nM primers (100~ 400 nM in optimization studies), 100 nM TaqMan probe (100~500 nM after optimization) was applied for each of the target genes. The accumulated fluorescent PCR products were measured by AB 7500 system and continuous monitoring. We carried out experiments in triplicate with no template control and no-RT sample.

2.12 Experiment of CRISPR-Cas13 system

All procedures followed from previous publication[46]. To mimic RNA A-to-I editing in vivo, we applied CRISPR method to guide ADAR1 to the designated loci to perform A-to-I editing. In brief, ADAR1 was fused with dCas13b and the corresponding crRNAs (crRNAs) were expressed in HEK-293T cells by transfecting pC0047-CMV-dPspCas13b-ADAR1DD (E1008Q) (Addgene no. 103863), RhoA_variant3 (isoform 2)_176_codon_crRNA contained pC0043-PspCas13b crRNA backbone (construct from Addgene no.103854), and pC0052-REPAIR non-targeting guide clone as negative control (Addgene no.103868). After 48 hours, RNA was collected and evaluated the A-to-I RNA editing efficacy by Taqman qPCR after cDNA synthesis. The sequence of RhoA_variant3(isoform2)_176_codon_crRNAs 5'-CACCGTCCTGAGTAGCTGGGGTTACGTTTT-3' designed by using PrimeDesign

(<https://drugthatgene.pinellolab.partners.org/>)[47].



2.13 Knockdown with shRNAs and lentiviral infections to cells.

The ADAR1 shRNAs (small hairpin RNAs) were obtained from the core facility of the TRC library: TRCN0000050788 (shRNA1) and TRCN0000050790 (shRNA2) from the National RNAi Core Facility Platform of Academia Sinica. The vectors of pLKO.1 with shRNAs, pMD2.G and psPAX2 were transfected into 293T host cells by turbofect for virus production. The viral supernatants were collected after 48 hours infection in A549 cell.




Chapter 3 Results

3.1 A-to-I RNA editing events were identified in LUAD patient transcriptomes

By comparing RNA transcripts to reference DNA sequence (hg19), we aimed to find out tumor specific A-to-I RNA edited events, where somatic mutations only occurred on the tumor but not on adjacent normal (Figure1). We first downloaded RNA-seq data derived from 23 LUAD patients with transcriptomes in both normal and tumor tissues from NCBI (GSE40419), then, we established a pipeline (Figure 2) for comprehensive identification of somatic RNA editing events. Reads with quality value (Q score) higher than 30 were collected, and each read contained 87 base pairs for reads quality control. The first 14 bases of each transcript read were cut due to inconsistent per base sequence content.

Furthermore, due to the difficulty of collecting the patients' genomic DNA and RNA sequencing data at the same time on the public domain, we therefore aligned sequence reads of normal and tumor samples to the reference genome (hg19) respectively by using STAR Aligner. We removed duplicate reads and kept the best quality of each unique read for further analysis. Normal and tumor reads alignments were processed with SAMtools followed by subsequently VarScan for the discovery of potential A-to-I editing sites. The known SNPs were removed according to the dbSNP database.

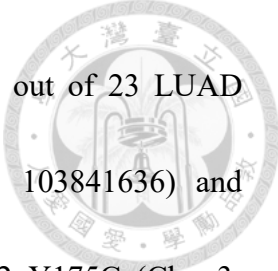


More than 52,000 candidate editing sites were identified with validation through two RNA editing databases (RADAR and DARNED), repetitive regions of editing sites were tagged based on UCSC RepeatMasker, and every editing site was annotated by gene symbols in accordance with GENCODE v19.

Consistence with previous studies, A-to-G and T-to-C edited events were the most common mismatch editing events out of the obtained 26,000 A-to-I RNA editing events (Figure 3 and Table 1). The result also showed that the majority of A-to-I RNA editing events resided in intronic and UTR regions among them 55% of RNA editing events detected in the Alu region (Figure 4), similar to previous research.

When further assessing the frequency and distribution of 26,000 RNA editing events in 23 LUAD patients, more than 90% of A-to-I editing events were existed in only 1/23 LUAD patients but three A-to-I editing events in the UTR regions, including PPIA (peptidylprolyl isomerase A, Chr.7: 44842099), SCD (stearoyl- CoA desaturase, Chr.10: 102121601), and MDM2(Chr. 12: 69237004) were identified in 11/23 LUAD patients (Figure 5). MDM2 was discovered to be a hyper-editing gene in cancer types in previous studies. A-to-I RNA editing site on on 3'UTR of MDM2 might regulate epithelial to mesenchymal transition (EMT)-related miR200.

To identify the potential therapeutic targets of A-to-I editing events occurring in the coding sequences (CDS) and possibly causing nonsynonymous mutations in lung




adenocarcinoma, we identified several events existed in 3–4 cases out of 23 LUAD patients including AZIN1-S367G (antizyme inhibitor 1, Chr. 8: 103841636) and RhoAiso2-R176G (RhoA isoform 2, Chr. 3: 49398382), RhoAiso2–Y175C (Chr. 3: 49398382), TUBGCP2-N211S (Chr. 10:135110893), and RBMXL1 (RNA binding motif protein, X-linked like 1-I40 M, Chr. 1: 89449390) mutations. We then further validated these nonsynonymous mutations in multiple A-to-I RNA editing databases (Figure 5) and in cancers of TCGA datasets. The results seemed to indicate that RhoAiso2-R176G had higher edited samples in tumor samples comparing to normal samples. Besides, we also found AZIN1, which was the first gene identified hyper-editing in two editome databases and associated with tumorigenesis of Hepatocellular carcinoma (HCC) in previous studies. The A-to-I RNA editing events occurred in the coding region of AZIN1 with amino acid changed from serine to glycine, therefore increasing high binding affinity with Antizyme which inhibited oncogenic ODC and CCND1 degradation to increased HCC progression. Thus, AZIN1, MDM2, and other four nonsynonymous A-to-I edited events were served as our validated targets. In summary, we identified 5 A-to-I RNA edited nonsynonymous mutations highly enriched in LUAD patients. With our stringent criteria, we believed that the identified 5 A-to-I edited nonsynonymous mutations might play important roles in LUAD tumorigenesis.


3.2 Validation of *in silico* identified somatic A-to-I RNA editing events with SEQUENOM MassARRAY® System in LUAD patient samples



We selected six somatic A-to-I editing events including 4 nonsynonymous AI-edited mutations and 2 3'UTR editing sites in LUAD for experimental validation at LUAD patient samples. We prepared both cDNAs and genomic DNAs from LUAD tumors and their corresponding adjacent normal tissues (n = 20) in Taiwan and 5 LUAD cell lines both cDNA and genomic DNA. In previous studies, pyrosequencing was the predominant tool for validating A-to-I editing sites as it would present A versus G peak percentage. However, considering pyrosequencing is cost-intensive and time-consuming. We implemented the SEQUENOM MassARRAY® System method to validate A-to-I RNA editing events. Said method is efficient and highly reproducible; moreover, it detects multiple sites simultaneously and can be performed with very limited amount of samples. Most importantly, the A-to-I editing ratio can be quantified. With known editing sites AZIN1-S367G and MDM2-UTR as positive controls for the validation experiments (Figure 6), the result demonstrated that higher RNA editing frequency (editing ratio) in MDM2-UTR (UTR) (average 21%) and AZIN1-S367G (average of 5.4% was detected in LUAD cancer cell lines and tissues matching with previous reports. In addition, we measured the A-to-I RNA editing frequency of the remaining four selected novel somatic



A-to-I RNA editing events including RHOAiso2-R176G, TUBGCP2-N211S, RBMXL1-I40 M and PPIA-UTR occurred in 5 LUAD cell lines and 20 LUAD patients in Taiwan (Figure 7 and 8). Our results showed that the RNA editing ratio was higher in tumor compared with adjacent normal tissues (n = 20) which was also consistent with our previous results in LUAD cell lines. We found that the RNA editing ratio of RHOAiso2-R176G nonsynonymous mutation was significantly higher in both LUAD cell lines and the local LUAD tumor samples compared to their adjacent normal tissues (Figure 7 and 8). Thus, we investigated the roles of the RHOAiso2-R176G mutation in LUAD tumorigenesis. Among Rho family proteins, RHOA, Rac1, and Cdc42 are the best characterized Rho GTPases to act as important regulators of cytoskeleton dynamics, to potentiate downstream cell motility-related signaling, and to modulate diverse cell migration activities via the regulatory switch from the inactive form of GDP-bound state to the active form of GTP-bound state [48]. RhoA has at least 6 isoforms, the major form is the longest RhoA isoform 1 (193 amino acid) (Ensembl ID:ENST00000418115), while RHOAiso2-R176G editing site is located in unique sequence of RhoA isoform 2 (187 amino acid) (Ensembl ID: ENST00000422781). Furthermore, we assessed informational RhoA isoforms expression in both the GTEx and TCGA databases collected in the UCSC Xena (Figure 9). We noted that RhoA isoform1 and isoform 2 were ubiquitously expressed in multiple normal and cancer tissues. So far, there is no



functional and mechanistic studies of RHOAiso2 in biology- and diseases-related relevant documentations. Here, we made a primary structural comparison between RhoA isoform 1 (UniProt ID: P61586) and RhoA isoform 2 (UniProt ID: C9JX21). After sequence alignment, RhoA isoform 2 has an alternate 3' coding exon in the C-terminal domain which is the hypervariable domain in RhoA isoform 1, and conserves identical N-terminal domain core guanine nucleotide-binding (G-domain) and the insert domains responsible for GTP and GDP binding for conformational changes required for GTPase activity (Figure 11).

Interestingly, Interestingly, several A-to-I RNA editing sites were found in the coding region which led to nonsynonymous mutation locating on RhoA isoform 2 C-terminal domain, instead of on the major RhoA isoform 1 as mentioned in REDiportal and The Cancer Editome Atlas (Figure 10 and 11). In our study, we acknowledged that more than 55% of A-to-I editing events occurred in Alu repetitive element. Therefore, we conducted annotation of repeat masked regions in the 3' coding exon in C-terminal sequence of RhoA isoform 1 and RhoA isoform 2 by using RepeatMasker. We discovered that RhoA isoform 2 3' coding exon in C-terminal sequence could form an Alu repetitive element, but not RhoA isoform 1. This might explain why RhoA isoform 2 shows hyper-edited on 3' coding exon in C-terminal thru alternative splicing mechanism. We also found RhoAiso2-R176G is noted to have the highest editing frequency across tumor types in



The Cancer Editome Atlas and REDiportal.

Consistent with in silico results, we confirmed that the expression of RhoA isoform 1 was much higher expressed than that of RhoA isoform 2 in LUAD cell lines via RT-qPCR test. Furthermore, to assess the RNA editing frequency of RhoAiso2-R176G, we performed TaqMan PCR system platform by two RhoAiso2-R176G specific probes, and showed a similar trend of RNA editing frequency by using MassARRAY platform (Figure 12).

ADAR (adenosine deaminase acting on double stranded RNA) family is an A to I RNA editing enzyme which can bind double strand RNA and catalyze Adenosine to Inosine, and inosine can be recognized as Guanosine during translation. Here, we would like to examine whether RhoAiso2-R176G was RNA edited by ADAR1 in LUAD cell lines. We knocked down ADAR1 with shRNA and detected the RNA editing ratio of RhoAiso2-R176G mutation. The result indicated that RNA editing ratio of RhoAiso2-R176G mutation has decreased during ADAR1 knockdown (Figure 13), whereas being increased when we overexpressed Cas13b-fused ADAR1 with crRNA. Taken together, we applied MassARRAY® system platform to quantitate A-to-I RNA editing ratio and identified that RhoAiso2-R176G presents higher RNA editing ratio in LUAD cell lines and in patients. Also RhoA isoform 2 has hyperediting harbor on 3' coding exon in C-terminal, and RhoAiso2-R176G increased and diminished RNA editing due to ADAR1 expression.

Thus, we further explore the function and roles of somatic edited RhoAiso2-R176G mutation in tumor progression of LUAD.



3.3 Comparison of gene signatures between the RHOAiso2-R176G and RHOAiso2 expressing LUAD patient transcriptomes



We would like to know whether A-to-I edited mutation of RhoAiso2-R176G will change the protein structure and cause different functions compare to parental RhoA isoform 2.

We downloaded the RHOA isoform 2 protein fragment structure from the database. We predicted 3D protein structure for comparison by using I-TASSER software (Figure 14).

We found that the prediction protein structure of RhoAiso2-R176G didn't change the conformational structure after superimposing with RhoAiso2(Figure 14).

Next, we investigated whether the edited RhoAiso2-R176G variant in LUAD patients would induce different functions compared with that of parental RhoAiso2 in transcriptome analysis. We performed gene set enrichment analysis (GSEA) of differential expression genes by comparing retrieved transcriptomes of GSE40419 between RHOAiso2-R176G variant and RHOAiso2 expressing LUAD samples. Surprisingly, we found gene signatures were upregulated in Rho-GTPases activity, Lung cancer poor survival, cell migration, G2M checkpoint, and epithelial-mesenchymal transition (EMT) which correlated with phenotypes of cell proliferation, cell migration, poor clinical outcome, and Rho function pathway in expressed RhoAiso2-R176G LUAD patients respectively. (Figure 15).

To further confirm our results, we constructed the RHOAiso2-R176G or RHOAiso2 clones and expressed above transfectants in the LUAD cell lines A549 and CL1-5. The expression efficiency was detected by western blot and immunofluorescence (Figure 16).

Then, we quantified the expression of selected genes in each functional gene signature at RNA level by RT-qPCR assay. By comparing the expression changes of the 22 genes in all four gene signatures including 7 genes of RHOA functions, 8 genes of cell proliferation, 10 genes of cell migration, and 7 genes of clinical outcomes, we detected significantly upregulation in overexpressed RhoAiso2-R176G variant compared to that RhoAiso2 variant and mock control in A549 and CL1-5 cell line. But no significant difference in these 22 genes expression in overexpressed RhoAiso2 compared to Mock control (Figure 17). We also analyzed the distribution of present of RhoAiso2-R176G in our 20 LUAD patients by stages, the result shows that stages of patients with RhoAiso2-R176G from IA2 to IVA and over 70% of patients with late stages. Furthermore, the patients expressing RhoAiso2-R176G variant increases recurrence risk 2.5 times compared to that of RhoAiso2 (Figure 18). Together, expression of somatic RNA A-to-I edited nonsynonymous RHOAiso2-R176G variant might involve Rho GTPases activation and regulate lung cancer cell migration and proliferation lead to poor clinical outcome in LUAD patients. Our results indicated that expression of RhoAiso2-R176G plays an important role in LUAD tumor progression.



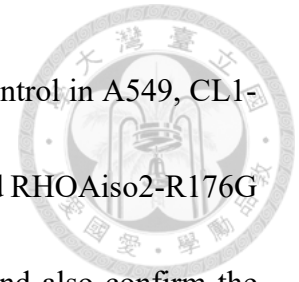


3.4 Expression of RHOAiso2-R176G increased cell proliferation and migration in

LUAD cells

To further investigate whether the expression of RHOAiso2-R176G variant might regulate cell growth and migration in LUAD cells *in vitro* and to confirm the GESA in LUAD patients' transcriptome and genes expression results in A549 and CL1-5 cell lines, we obtained RHOAiso2 and RHOAiso2-R176G stable clones in A549, CL1-5, and CL1-0 cell lines for further functional investigation. The expression efficiency was detected by western blot and immunofluorescence (Figure 16). We found that expression of RHOAiso2-R176G variant significantly increased cell growing capability in A549, CL1-5, and CL1-0 cell lines compared to that of RhoAiso2 (Figure 19 and 20). Since cell migration is involved in many pathological processes which might cause cancer metastasis, angiogenesis, immune response, and tumor progression that depends on cell motility speed and direction of cell migration, we studied the expressed RHOAiso2-R176G variant in cell migration and cell motility more quantitatively and at the single-cell level. Here, we demonstrated wound closure dynamics in 12h and 24h by wound healing assay, and the result showed cell migration was increased in A549, CL1-5, and CL1-0 expressed RhoAiso2-R176G compared to RhoAiso2 and Mock control. To assess the single-cell migration, we track of dozens of individual cells with expressed RhoAiso2-R176G, RhoAiso2 and Mock control over 24 hours series and revealed that cell migration

increased in RhoAiso2-R176G compared to RhoAiso2 and Mock control in A549, CL1-5 cell lines (Figure 19). Taken together, we suggest that the expressed RHOAiso2-R176G variant in LUAD cells increased cell proliferation and migration and also confirm the predicted GSEA functions from transcriptomes in LUAD patients.



3.5 Expression of RHOAiso2-R176G increased tumor growth and metastasis

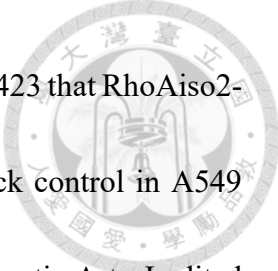


Next, we further investigated the RHOAiso2-R176G expression involved in tumor progression, and the orthotopic xenograft mouse model was performed as *in vivo* assays (Figure 21). We expressed the RhoAiso2-R176G and RhoAiso2 in CL1-5 cells mixed with Matrigel and subcutaneously injected into mice. As the results *in vivo*, RhoAiso2-R176G transfectant promoted tumor growth and tumor volume compared to that of RhoAiso2 in the orthotopic xenograft model. Later, orthotopic mouse model in systemic metastasis assays migrated to lung tissues was performed by mice tail vein injection, and the result showed increased tumor nodules in lung tissues in RhoAiso2-R176G variants group compared to RhoAiso2 group. We suggested that RHOAiso2-R176G variant has oncogenic feature and promote LUAD tumor progression *in vivo*.

3.6 Expression of RHOAiso2-R176G increased RHOA-GTP activity and downstream phosphorylated ROCK1/2 signaling



Since we confirmed expression of the RhoAiso2-R176G variant enhanced cell growth and migration *in vitro* and also increased tumor size and tumor metastasis *in vivo* in LUAD, we further investigate downstream oncogenic signaling activated by RhoAiso2-R176G. RhoA is a Small GTPase and activated RhoA can regulate cell migration, invasion, cell cycle, apoptosis, and angiogenesis by activated downstream effectors ROCK1/2 (Rho-associated, coiled-coil-containing protein kinase 1/2) which control multiple functions. Besides, RhoAiso2 has a different 3' coding exon in the C-terminal domain compared to RhoA isoform 1, and acts as an RNA editing harbor in RhoA isoform 2 C-terminal. Moreover, there is no mention any function of RhoA isoform 2 in literature. Thus, we would like to know whether RhoA isoform 2 also has GTPase function and will RhoAiso2-R176G gain or lose function compared to parental RhoA isoform 2. We, therefore, measured RhoA-GTP activity and downstream Rock1/2 phosphorylation in RhoAiso2-R176G compared to RhoAiso2 in A549 and CL1-5 cell lines treated with or without RhoA activator (Figure 22). The result showed that expression of RhoAiso2-R176G increased the active RhoA-GTP compared to that of parental RhoA isoform 2, and also increased phosphorylation Rock1/2 in A549 and CL1-5 with or without treated



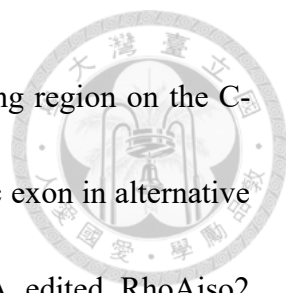
RhoA activator. Furthermore, when we treated RhoA inhibitor CCG-1423 that RhoAiso2-R176G also increased cell viability compared to RhoAiso2 and Mock control in A549 and CL1-5 (Figure 23). In summary, our results indicated that the somatic A-to-I edited RhoAiso2-R176G variant plays an oncogenic role and enhanced tumor progression in LUAD though increase of active form RhoA-GTP and downstream p-Rock1/2 signaling.

Chapter 4 Discussion and Conclusion



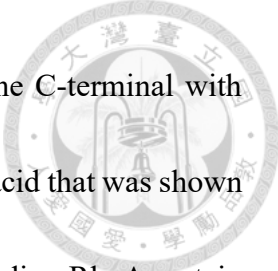
In this study, we identified 26,280 somatic A-to-I RNA editing events in transcriptomes derived from 23 paired LUAD patients, validated the known MDM2-UTR and AZIN1-S367G as our positive control, and uncovered the innovative (RHOAiso2-R176G, TUBGCP2-N211S, RBMXL1-I40M, and PPIA-UTR) RNA editing events in silico with editing data in databases and experimentally with SEQUENOM MassARRAY® System and Taqman system in LUAD patient samples and LUAD cell lines. Finally, we conducted functional assays to indicate that expression of RHOA isoform 2 specifically RHOAiso2-R176G variant is an oncogenic driver via upregulated RHOA-GTP/p-ROCK1/2 axis in tumor progression of LUAD cell and mice models. In addition to the common somatic therapeutic mutations detected at the genomic DNA level, our results added a new direction to identify cancer driver mutations from the somatic posttranscriptional A-to-I RNA edited nonsynonymous mutations that facilitate LUAD tumor progression.

Furthermore, we found RhoA isoform 2 has an A-to-I RNA editing hub harbored in the 3' exon coding region on the C-terminal domain, and only specific in RhoA isoform 2 but not in RhoA isoform1 thru alternative splicing. Due to the ADARs enzymatic feature which can covert adenosine to inosine on Alu repetitive regions, we conducted




investigation to know whether the Alu element in the 3' exon coding region on the C-terminal domain specific in RhoA isoform 2 after gaining the cryptic exon in alternative splicing. In our results, we identified three somatic A-to-I RNA edited RhoAiso2 nonsynonymous mutation in 23 paired LUAD patient transcriptomes including RhoAiso2-R176G, Y175C, and K162R with high RNA editing frequency in our result and also confirmed from REDportal and TCEA database. Moreover, we demonstrated that expression of RHOA isoform 2 specific RHOAiso2-R176G variant could enhance RhoA-GTPase activity in LUAD cell lines and further to increase cell proliferation and migration. At the same time, RhoAiso2-R176G expression also shows higher cell viability when RhoA inhibitor was treated compared to parental RhoA isoform2.

RhoA is a member of Rho GTPase family which was composed of Rac1, RhoA and Cdc42. RhoA was well-studied after it was discovered from 1980s. In addition, RhoA was shown to participate in many functional mechanisms to regulate cell cycle, actin organization and cell adhesion.[27]. The RhoA protein has five alternative variants including isoform 1 (193 amino acids and 22 kDa) which is the longest variant , isoform 2 (187 amino acids, similar molecular weight to isoform 1) , isoform 3 (90 amino acids), isoform 4 (129 amino acids) and isoform 5 (86 amino acids) (Figure 9). The functional and primary structural data demonstrated that RhoA is composed of effector binding



domain, GTP or GDP binding domain, hypervariable domain and the C-terminal with CAAX motif. The hypervariable region located from 173-189 amino acid that was shown to have the most diversity region among RhoA variants. In previous studies, RhoA protein translocated from membrane to nucleus was regulated by palmitoylation on the C-terminus of RhoA, which regulated many biological functions.[49] The hypervariable region and C-terminus are involved in regulatory or effector protein binding when C-terminus undergoes post-translational lipid modification. In our study, we validated the expression RhoA isoform 2-specific RNA edited nonsynonymous mutations which occur on A-to-I RNA editing harbor with enhanced oncogenic functions. However, the mechanism of RhoAiso2-R176G enhanced GTPase activity is still unknown. In the coming future, we would like to know whether A-to-I RNA editing events that occur in RhoA isoform 2 harbor will have other biological meaning in LUAD tumor progression such as regulating C-terminus geranylgeranylation or modulating RhoA subcellular localization.

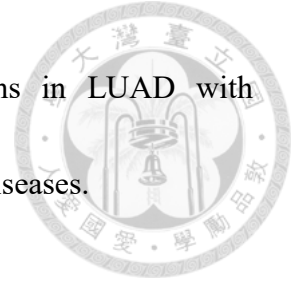
However, although there are millions of A-to-I RNA editing events reported, the function and mechanisms involved in cancer progression of A-to-I editing events were still rarely explored. For instance, AZIN1-S367G variant is the well-discovered A-to-I edited mutation with more affinity to antizyme, a protease to degrade cell cycle proteins such as ornithine decarboxylase (ODC1) and cyclin D1 (CCND1), to enhance cell growing



capability and tumor growth. MDM2-UTR is another known A-to-I RNA editing variant at the 3'-UTR MDM2 that could interfere with the microRNA-155 binding to stabilize MDM2 transcripts and enhance cell proliferation. In our study, we provided a new insight that A-to-I edited nonsynonymous somatic mutation RHOAiso2-R176G could be prioritized for functional evaluation and develop a therapeutic target against LUAD tumor progression. In addition, our preliminary but yet to reconfirm result also found RhoAiso2-R176G might potentially regulate cell migration and proliferation through activated FAK/SPP1 axis.

In conclusion, 26,280 somatic posttranscriptional A-to-I RNA editing events were identified in transcriptomes of 23 paired LUAD and validated the frequent nonsynonymous A-to-I edited variant sites in silico in multiple cancers in TCGA datasets and with the SEQUENOM MassARRAY® System by using the locally collected twenty cases of LUAD pair samples. After functional validations of somatic A-to-I RNA edited nonsynonymous RHOAiso2-R176G variant in LUAD *in vitro* and *in vivo* models, we showed that RHOAiso2-R176G expression could activate downstream RHOA-GTP/p-ROCK1/2 signaling to facilitate LUAD tumor progression. Referring to the high percentage of LUAD patients expressing RHOAiso2-R176G variant, it might be a nonnegligible therapeutic target in LUAD with isoform specific targeting strategies. Our results established a new avenue to identify innovative theranostic targets vis

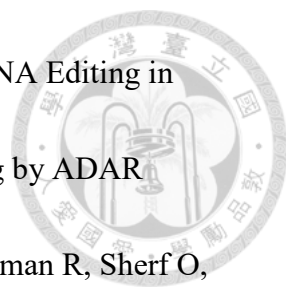
posttranscriptional A-to-I RNA edited nonsynonymous mutations in LUAD with potential therapeutic and diagnostic impacts to cancers and human diseases.



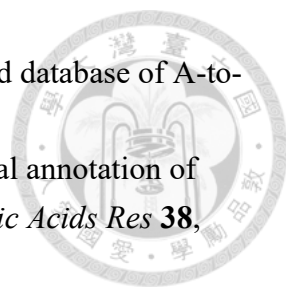


Reference

- [1] Siegel RL, Miller KD, Fuchs HE, Jemal A (2022). Cancer statistics, 2022 *CA Cancer J Clin* **72**, 7-33.
- [2] Myers DJ, Wallen JM (2022). *Lung Adenocarcinoma: Treasure Island (FL)*.
- [3] Sun S, Schiller JH, Gazdar AF (2007). Lung cancer in never smokers--a different disease *Nat Rev Cancer* **7**, 778-790.
- [4] Lynch TJ, Bell DW, Sordella R, Gurubhagavatula S, Okimoto RA, Brannigan BW, Harris PL, Haserlat SM, Supko JG, Haluska FG, et al. (2004). Activating mutations in the epidermal growth factor receptor underlying responsiveness of non-small-cell lung cancer to gefitinib *N Engl J Med* **350**, 2129-2139.
- [5] Paez JG, Jänne PA, Lee JC, Tracy S, Greulich H, Gabriel S, Herman P, Kaye FJ, Lindeman N, Boggon TJ, et al. (2004). EGFR mutations in lung cancer: correlation with clinical response to gefitinib therapy *Science* **304**, 1497-1500.
- [6] Soda M, Choi YL, Enomoto M, Takada S, Yamashita Y, Ishikawa S, Fujiwara S-i, Watanabe H, Kurashina K, Hatanaka H, et al. (2007). Identification of the transforming EML4-ALK fusion gene in non-small-cell lung cancer *Nature* **448**, 561-566.
- [7] Pardoll DM (2012). The blockade of immune checkpoints in cancer immunotherapy *Nat Rev Cancer* **12**, 252-264.
- [8] Topalian SL, Hodi FS, Brahmer JR, Gettinger SN, Smith DC, McDermott DF, Powderly JD, Carvajal RD, Sosman JA, Atkins MB, et al. (2012). Safety, activity, and immune correlates of anti-PD-1 antibody in cancer *N Engl J Med* **366**, 2443-2454.
- [9] Rizvi NA, Hellmann MD, Snyder A, Kvistborg P, Makarov V, Havel JJ, Lee W, Yuan J, Wong P, Ho TS, et al. (2015). Cancer immunology. Mutational landscape determines sensitivity to PD-1 blockade in non-small cell lung cancer *Science* **348**, 124-128.
- [10] de Miguel M, Calvo E (2020). Clinical Challenges of Immune Checkpoint Inhibitors *Cancer Cell* **38**, 326-333.
- [11] Haslam A, Prasad V (2019). Estimation of the Percentage of US Patients With Cancer Who Are Eligible for and Respond to Checkpoint Inhibitor Immunotherapy Drugs *JAMA network open* **2**, e192535.
- [12] Marquart J, Chen EY, Prasad V (2018). Estimation of the Percentage of US Patients With Cancer Who Benefit From Genome-Driven Oncology *JAMA oncology* **4**, 1093-1098.

- 
- [13] Baysal BE, Sharma S, Hashemikhabir S, Janga SC (2017). RNA Editing in Pathogenesis of Cancer *Cancer Res* **77**, 3733-3739.
- [14] Nishikura K (2010). Functions and regulation of RNA editing by ADAR deaminases *Annu Rev Biochem* **79**, 321-349.
- [15] Osenberg S, Paz Yaacov N, Safran M, Moshkovitz S, Shtrichman R, Sherf O, Jacob-Hirsch J, Keshet G, Amariglio N, Itskovitz-Eldor J, et al. (2010). Alu sequences in undifferentiated human embryonic stem cells display high levels of A-to-I RNA editing *PLoS One* **5**, e11173.
- [16] Greenberger S, Levanon EY, Paz-Yaacov N, Barzilai A, Safran M, Osenberg S, Amariglio N, Rechavi G, Eisenberg E (2010). Consistent levels of A-to-I RNA editing across individuals in coding sequences and non-conserved Alu repeats *BMC Genomics* **11**, 608.
- [17] Ramaswami G, Lin W, Piskol R, Tan MH, Davis C, Li JB (2012). Accurate identification of human Alu and non-Alu RNA editing sites *Nat Methods* **9**, 579-581.
- [18] Wang H, Chen S, Wei J, Song G, Zhao Y (2020). A-to-I RNA Editing in Cancer: From Evaluating the Editing Level to Exploring the Editing Effects *Front Oncol* **10**, 632187.
- [19] Aquino-Jarquín G (2020). Novel Engineered Programmable Systems for ADAR-Mediated RNA Editing *Mol Ther Nucleic Acids* **19**, 1065-1072.
- [20] Reardon S (2020). Step aside CRISPR, RNA editing is taking off *Nature* **578**, 24-27.
- [21] Liu L, Pei DS (2022). Insights Gained from RNA Editing Targeted by the CRISPR-Cas13 Family *International journal of molecular sciences* **23**.
- [22] Wang JY, Pausch P, Doudna JA (2022). Structural biology of CRISPR–Cas immunity and genome editing enzymes *Nature Reviews Microbiology* **20**, 641-656.
- [23] Kiran A, Baranov PV (2010). DARNED: a DAtabase of RNa EDiting in humans *Bioinformatics* **26**, 1772-1776.
- [24] Picardi E, D'Erchia AM, Lo Giudice C, Pesole G (2017). REDiportal: a comprehensive database of A-to-I RNA editing events in humans *Nucleic Acids Res* **45**, D750-d757.
- [25] Lin CH, Chen SC (2019). The Cancer Editome Atlas: A Resource for Exploratory Analysis of the Adenosine-to-Inosine RNA Editome in Cancer *Cancer Res* **79**, 3001-3006.
- [26] Sahai E, Marshall CJ (2002). RHO-GTPases and cancer *Nat Rev Cancer* **2**, 133-142.
- [27] Madaule P, Axel R (1985). A novel ras-related gene family *Cell* **41**, 31-40.

- 
- [28] Schmidt SI, Blaabjerg M, Freude K, Meyer M (2022). RhoA Signaling in Neurodegenerative Diseases *Cells* **11**.
- [29] Crosas-Molist E, Samain R, Kohlhammer L, Orgaz JL, George SL, Maiques O, Barcelo J, Sanz-Moreno V (2022). Rho GTPase signaling in cancer progression and dissemination *Physiological Reviews* **102**, 455-510.
- [30] Nam S, Lee Y, Kim JH (2022). RHOA protein expression correlates with clinical features in gastric cancer: a systematic review and meta-analysis *BMC Cancer* **22**, 798.
- [31] van Unen J, Botman D, Yin T, Wu YI, Hink MA, Gadella TWJ, Postma M, Goedhart J (2016). Palmitoylation of the oncogenic RhoGEF TGAT is dispensable for membrane localization and consequent activation of RhoA *bioRxiv*, 062729.
- [32] Ungefroren H, Witte D, Lehnert H (2018). The role of small GTPases of the Rho/Rac family in TGF-beta-induced EMT and cell motility in cancer *Developmental dynamics : an official publication of the American Association of Anatomists* **247**, 451-461.
- [33] Deng Z, Jia Y, Liu H, He M, Yang Y, Xiao W, Li Y (2019). RhoA/ROCK pathway: implication in osteoarthritis and therapeutic targets *Am J Transl Res* **11**, 5324-5331.
- [34] Svensmark JH, Brakebusch C (2019). Rho GTPases in cancer: friend or foe? *Oncogene* **38**, 7447-7456.
- [35] Seo JS, Ju YS, Lee WC, Shin JY, Lee JK, Bleazard T, Lee J, Jung YJ, Kim JO, Shin JY, et al. (2012). The transcriptional landscape and mutational profile of lung adenocarcinoma *Genome Res* **22**, 2109-2119.
- [36] Bolger AM, Lohse M, Usadel B (2014). Trimmomatic: a flexible trimmer for Illumina sequence data *Bioinformatics* **30**, 2114-2120.
- [37] Smit A, Hubley, R & Green, P. (2013-2015). *RepeatMasker Open-4.0*. . Editor (ed)^(eds): City.
- [38] Dobin A, Davis CA, Schlesinger F, Drenkow J, Zaleski C, Jha S, Batut P, Chaisson M, Gingeras TR (2013). STAR: ultrafast universal RNA-seq aligner *Bioinformatics* **29**, 15-21.
- [39] Koboldt DC, Zhang Q, Larson DE, Shen D, McLellan MD, Lin L, Miller CA, Mardis ER, Ding L, Wilson RK (2012). VarScan 2: somatic mutation and copy number alteration discovery in cancer by exome sequencing *Genome Res* **22**, 568-576.
- [40] Sherry ST, Ward MH, Kholodov M, Baker J, Phan L, Smigielski EM, Sirotkin K (2001). dbSNP: the NCBI database of genetic variation *Nucleic Acids Res* **29**, 308-311.

- 
- [41] Ramaswami G, Li JB (2014). RADAR: a rigorously annotated database of A-to-I RNA editing *Nucleic Acids Res* **42**, D109-113.
- [42] Wang K, Li M, Hakonarson H (2010). ANNOVAR: functional annotation of genetic variants from high-throughput sequencing data *Nucleic Acids Res* **38**, e164.
- [43] Subramanian A, Tamayo P, Mootha VK, Mukherjee S, Ebert BL, Gillette MA, Paulovich A, Pomeroy SL, Golub TR, Lander ES, et al. (2005). Gene set enrichment analysis: A knowledge-based approach for interpreting genome-wide expression profiles *Proceedings of the National Academy of Sciences* **102**, 15545-15550.
- [44] Yang J, Zhang Y (2015). I-TASSER server: new development for protein structure and function predictions *Nucleic Acids Res* **43**, W174-181.
- [45] Yang J, Yan R, Roy A, Xu D, Poisson J, Zhang Y (2015). The I-TASSER Suite: protein structure and function prediction *Nat Methods* **12**, 7-8.
- [46] Cox DBT, Gootenberg JS, Abudayyeh OO, Franklin B, Kellner MJ, Joung J, Zhang F (2017). RNA editing with CRISPR-Cas13 *Science* **358**, 1019-1027.
- [47] Hsu JY, Grünewald J, Szalay R, Shih J, Anzalone AV, Lam KC, Shen MW, Petri K, Liu DR, Joung JK, et al. (2021). PrimeDesign software for rapid and simplified design of prime editing guide RNAs *Nature Communications* **12**, 1034.
- [48] Hodge RG, Ridley AJ (2016). Regulating Rho GTPases and their regulators *Nature reviews Molecular cell biology* **17**, 496-510.
- [49] Xu J, Li Y, Yang X, Chen Y, Chen M (2013). Nuclear translocation of small G protein RhoA via active transportation in gastric cancer cells *Oncol Rep* **30**, 1878-1882.





(A)

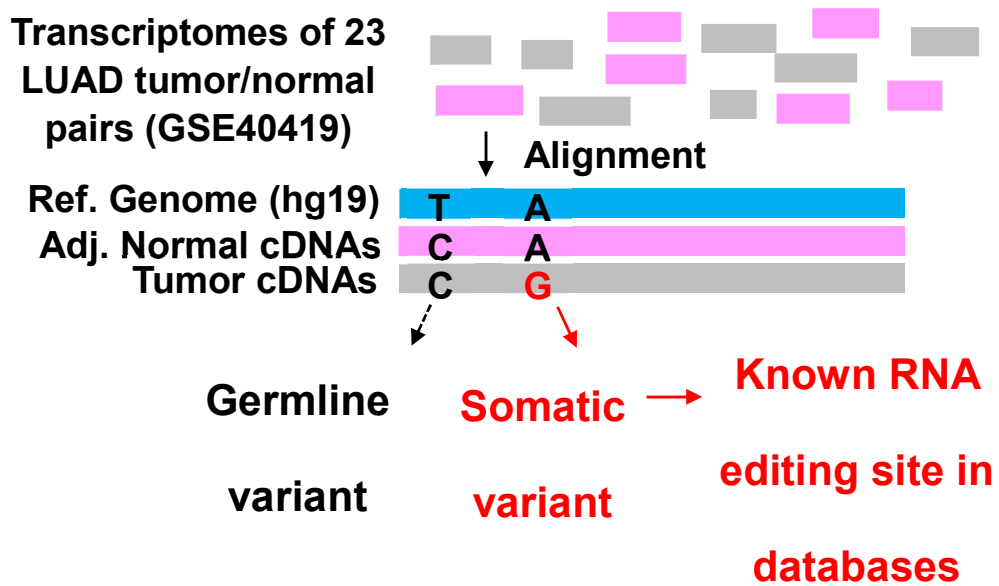


Figure 1 The schematic drawing of identifying A-to-I RNA editing events in LUAD transcriptomes with tumor and the corresponding normal pair.



(A)

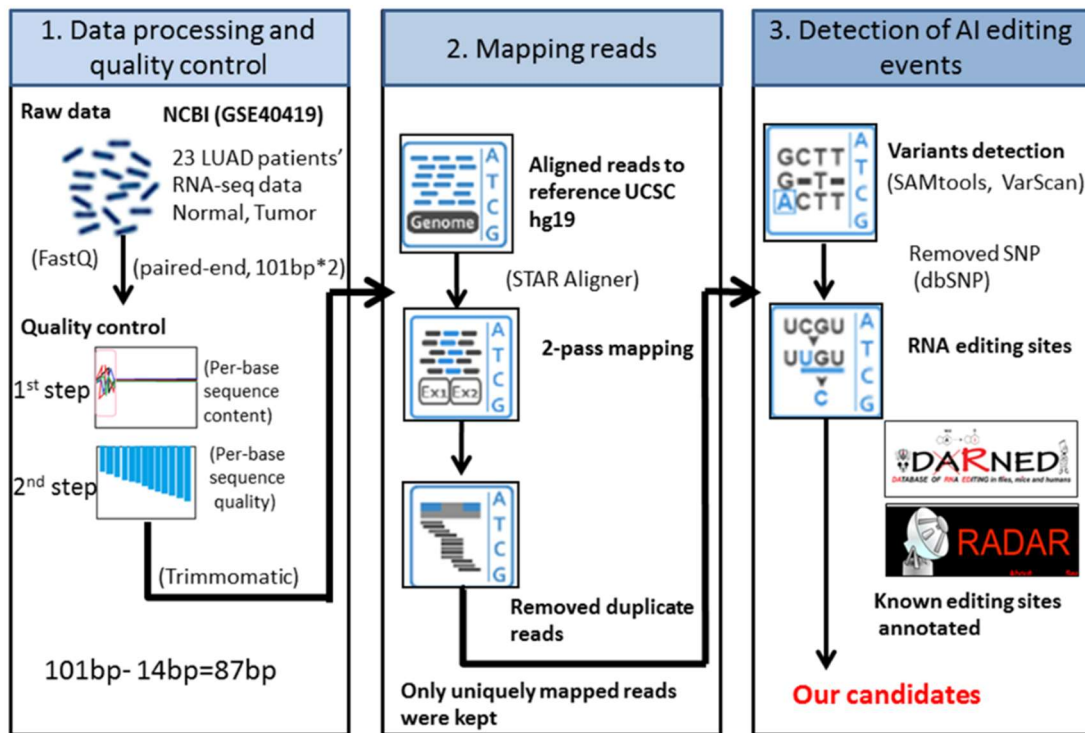


Figure 2 The detail pipeline for identification of genome-wide A-to-I editing events of LUAD transcriptomes and validation in the known editing databases in silico.



(A)

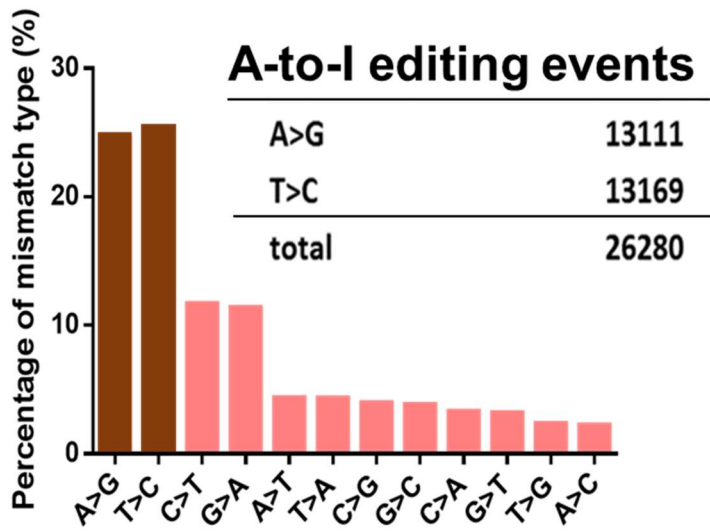


Figure 3 RNA mismatch types.

(A) A > G and T > C were the most common types of mismatch editing events



(A)

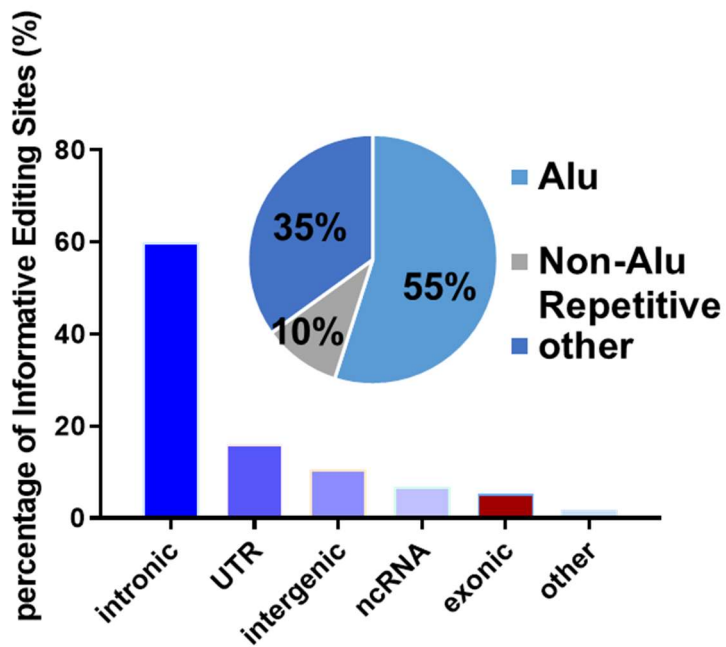
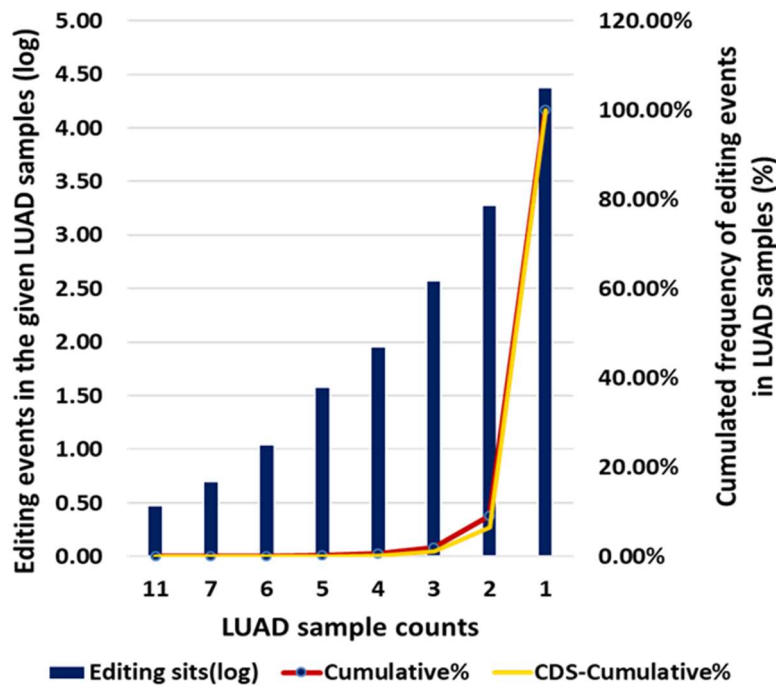


Figure 4 Identify the region of informative editing sites.

(A) The majority of A-to-I RNA editing events resided in intronic and UTR regions, and approximately 55% of RNA editing events occurred in the Alu region



(A)



LUAD Sample counts (out of 23 LUADs)	11	7	6	5	4	3	2	1
Editing events in the given LUAD samples (log)	0.48	0.70	1.04	1.58	1.96	2.57	3.28	4.38
Cumulated All editing frequency %	0.01%	0.03%	0.07%	0.22%	0.56%	1.99%	9.16%	100.00%
Cumulated CDS editing frequency %	0%	0%	0%	0%	0.18%	1.21%	6.59%	100%

(B)

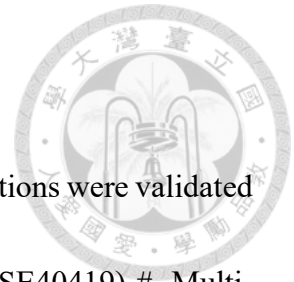
Gene	Position (hg19)	Edited samples*	Amino acid changed	Editome Databases		Editing events in cancers [#]	
				DARNED	REDportal (Edited samples)	TCGA_All (T/N)	TCGA_LUAD (T/N)
AZIN1	Chr8:103841636	4/23	S367G	Yes	9100	9773/703	526/59
RHOA	Chr3:49398382	3/23	R176G	Yes	8553	3981/286	367/36
RHOA	Chr3:49398384	3/23	Y175C	Yes	8126	2739/165	339/34
TUBGCP2	Chr10:135110893	4/23	N211S	No	6331	387/11	41/1
RBMXL1	Chr1:89449390	3/23	I40M	No	-	-	-

Figure 5 The sample counts of RNA editing events in 23 LUAD patients.

(A) The RNA editing frequency of total editing events in LUAD samples (n = 23, GSE40419). The cumulative editing events marked in blue; the frequency of cumulative total editing marked in red and the percentage of editing events in coding sequences (CDS)

marked in yellow.

(B) Selected five A-to-I RNA editing events of nonsynonymous mutations were validated in the Editome and TCGA databases.*, LUAD samples (n = 23, GSE40419) #, Multi-cancer types in TCGA and the LUAD samples from TCGA data.



(A)

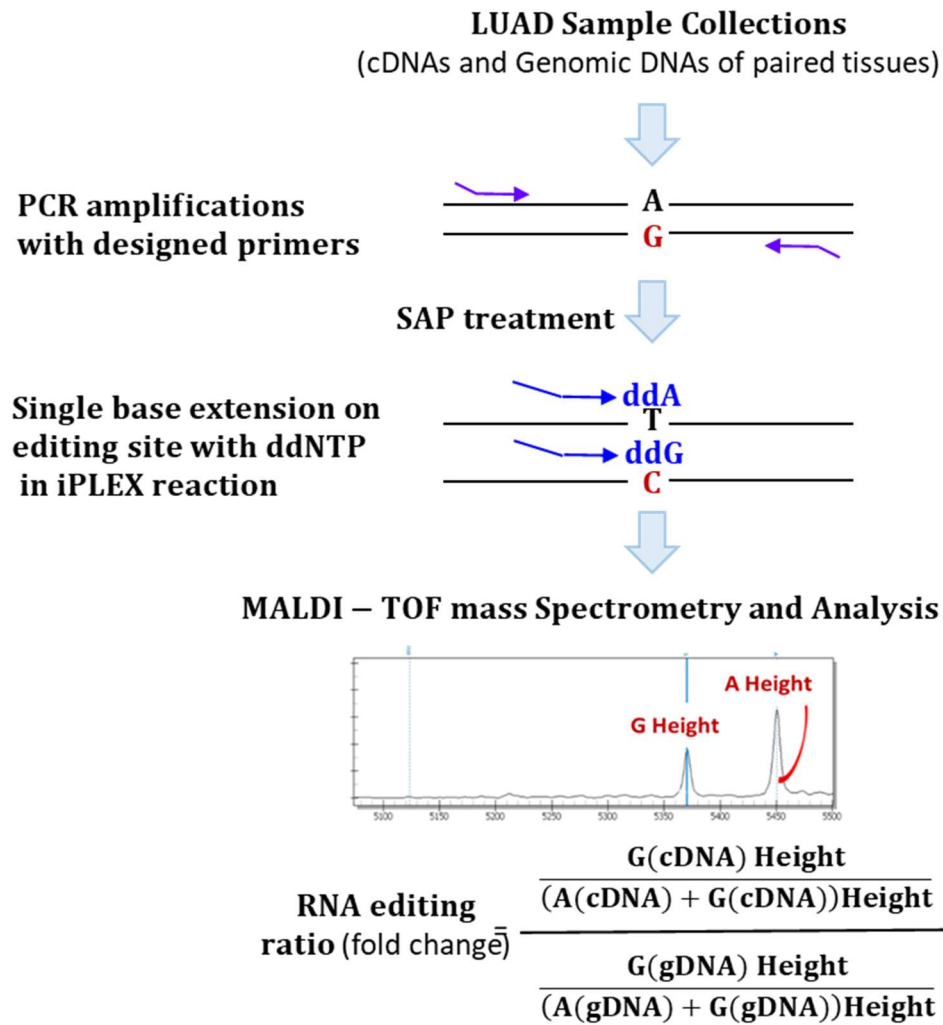


Figure 6 SEQUENOM MassARRAY® System method to validate A-to-I RNA editing extents and editing ratio formula.

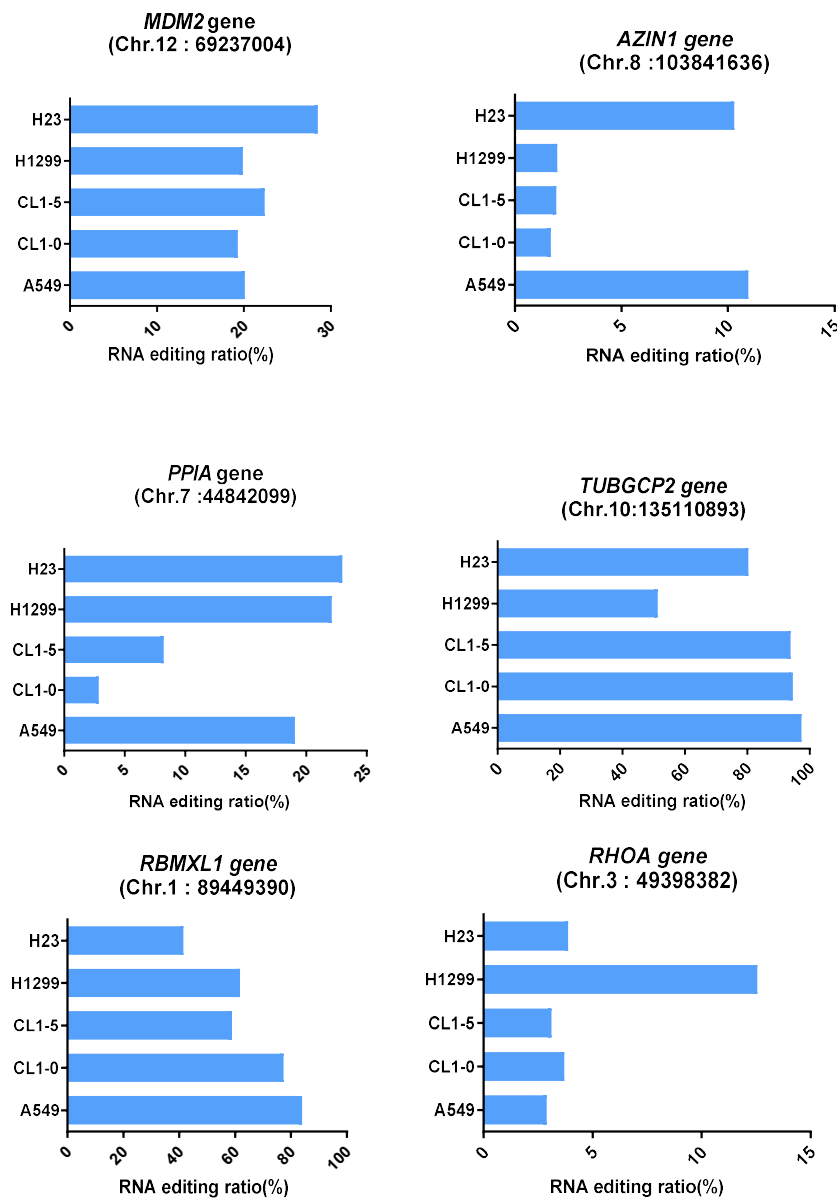


Figure 7 The RNA editing frequency of Selected A-to-I RNA editing sites in LUAD cell lines

The MDM2 and AZIN1 editing sites served as positive controls for the A-to-I RNA editing events located in the noncoding UTR and the nonsynonymous mutations, respectively. AZIN1 (Chr.8: 103841636), MDM2 (Chr.12: 69237004), PPIA (Chr.7:

44842099), TUBGCP2 (Chr.10 135110893), RBMXL1 (Chr.1 89449390), and RHOA
(Chr.3 49398382) candidate genes.



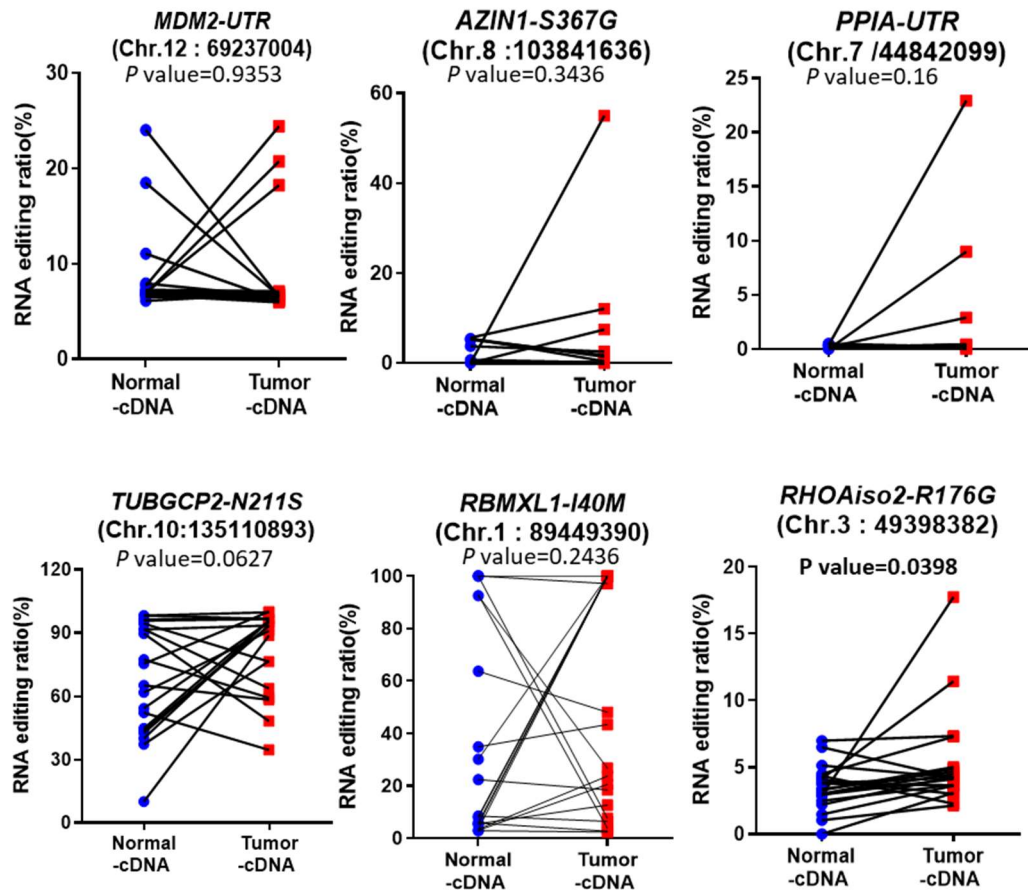


Figure 8 The RNA editing frequency of Selected A-to-I RNA editing sites in paired LUAD samples(n=20).

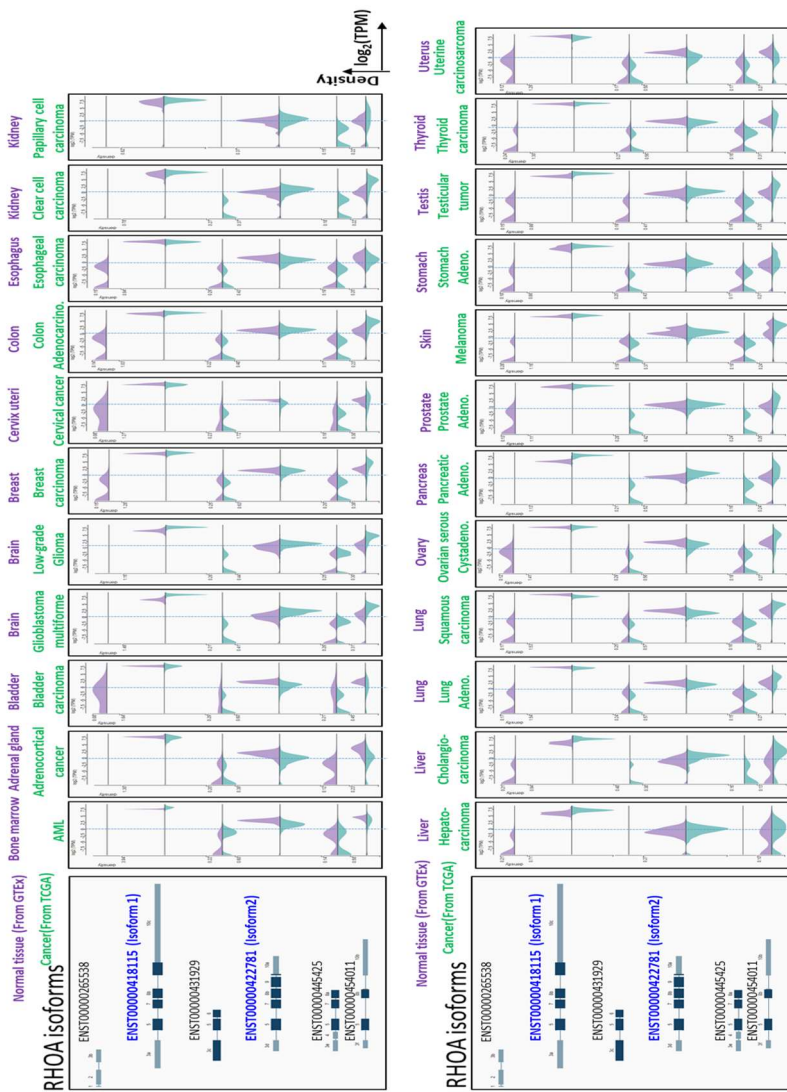


Figure 9 Expression of RHOA alternative splicing isoforms in normal (GTEx) and cancer (TCGA) tissues in UCSC Xena.

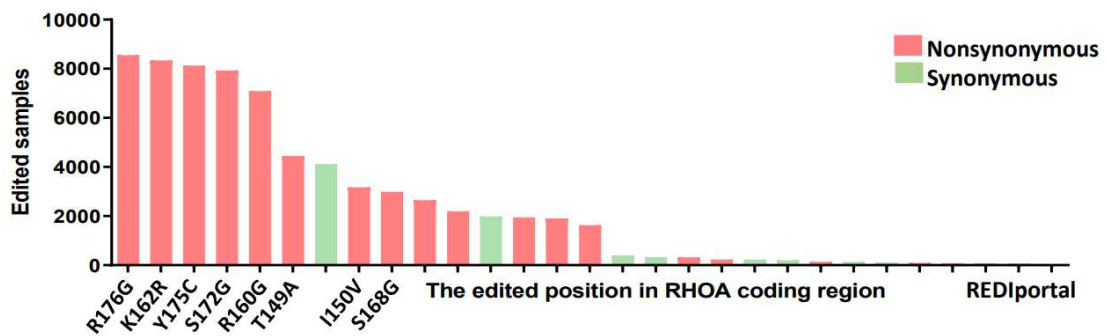
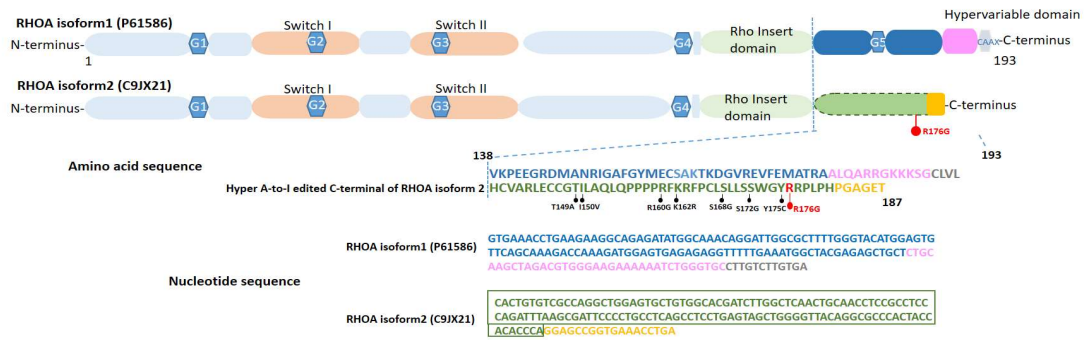


Figure 10 Nonsynonymous A-to-I RNA editing sites preferentially located at the unique C-terminal of RHOA isoform 2 but not the major isoform 1 of RHOA.



(A)



(B)

	RhoA isoform1 (P61586:139-193)	RhoA isoform2 (C9JX21:139-187)
Total nucleotide length (In C-terminal)	168bp	150bp
ALU position (In Amino acid sequence)	N/A	139-182
Repeat family		SINE/Alu

Figure 11 The schematic drawing of RhoA isoform 1 and 2 domains.

(A) Made a comparison between RhoA isoform 1 (UniProt ID: P61586) and RhoA isoform 2 (UniProt ID: C9JX21). The RHOA isoform 2 seems a hyper A-to-I edited events harbor instead of the RHOA major isoform 1.

(B) The C-terminal of RhoAiso2 was Alu element rich region.

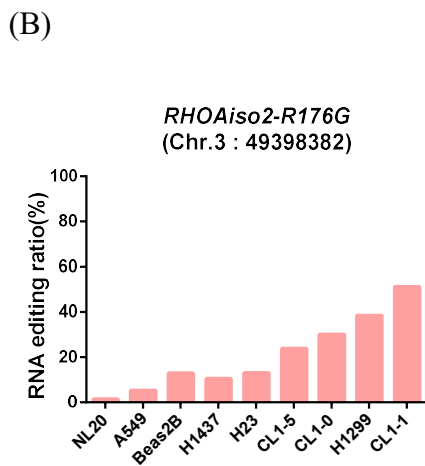
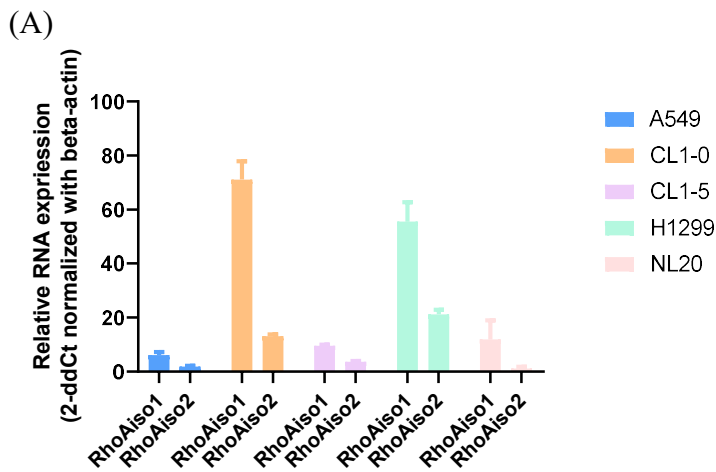


Figure 12 Expression of RHOA isoforms and RHOAiso2-R176G in LUAD cell

lines by using TaqMan platforms.

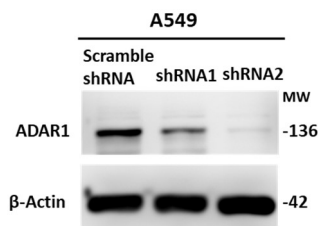
(A) Expression of RHOA isoforms 1 and 2 in LUAD cell lines by using RT-qPCR. (B)

Detection of RHOAiso2-R176G A-to-I RNA editing ratio (%) in LUAD cell lines with

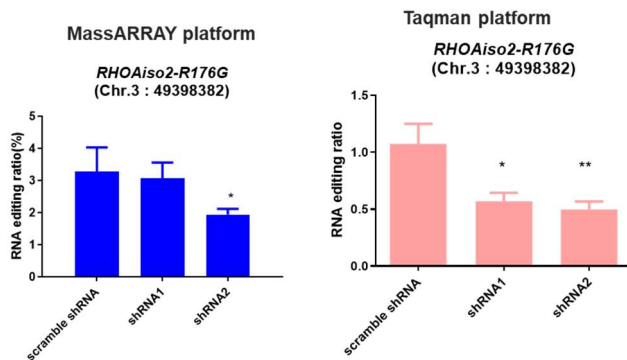
TaqMan platforms



(A)



(B)



(C)

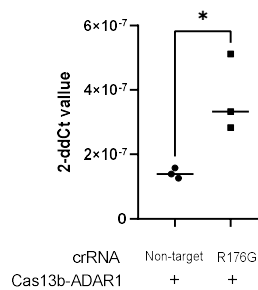


Figure 13 ADAR1 expression modulates A-to-I RNA editing led to RHOAiso2-R176G mutation.

(A) Knocked down ADAR1 with shRNAs diminished expression of ADAR1 at protein

level by Western blotting analysis led to reduced A-to-I RNA editing ratios of

RHOAiso2-R176G in A549 cells by using MassARRAY and TaqMan Platforms.

(B) Overexpression of Cas13b-fused ADAR1 and R176G corresponding crRNA elevated

A-to-I RNA editing of RHOAiso2-R176G mutation in 293T cell.



(B) Predicted 3D structure of RHOAiso2 -R176G(position indicated by red arrow).

(C) Predicted RHOAiso2 (blue) 3D structure superimposed with predicted RHOAiso2-

R176G (pink) 3D structure (red arrow indicating R176G position)





**Functional Enrichments in LUAD transcriptomes of GSE40419
RHOAiso2-R176G patients (n=3) / None RHOAiso2-R176G patients (n=20)**

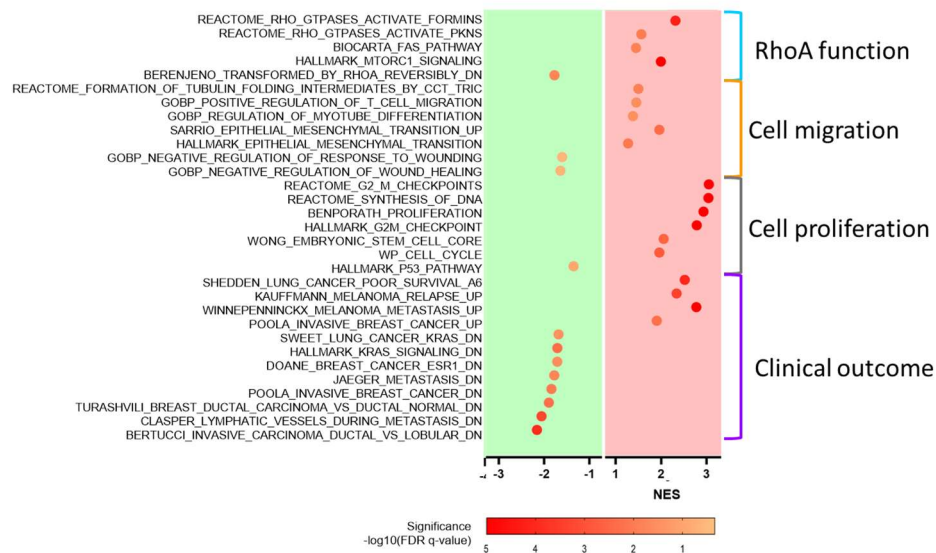
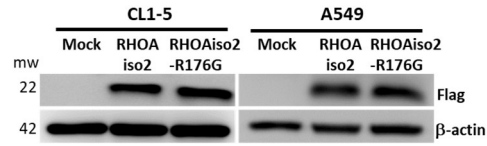
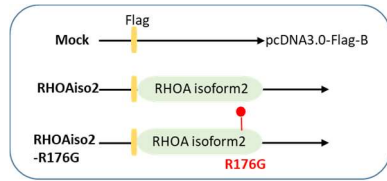


Figure 15 Comparison of gene signatures between the RHOAiso2-R176G and RHOAiso2 expressing LUAD patient transcriptomes

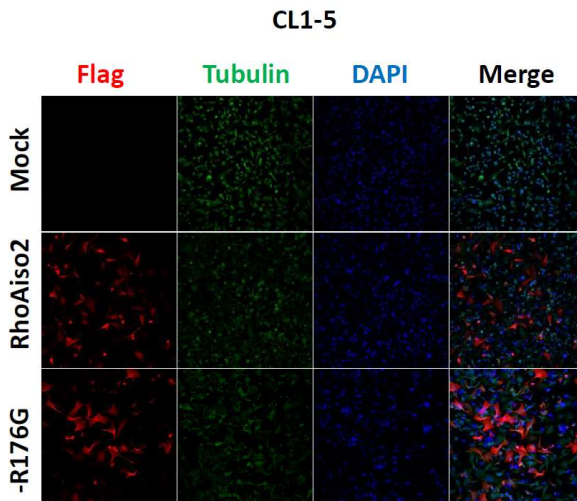
Gene set enrichment analysis (GSEA) of differential expression genes by comparing between RHOAiso2-R176G variant and RHOAiso2 expressing LUAD transcriptomes (GSE40419). The gene signatures were upregulated in Rho-GTPases activate, Lung cancer poor survival, cell migration, G2M checkpoint, and epithelial-mesenchymal transition (EMT) which correlated with cell proliferation (marked in gray), cell migration (marked in brown), poor clinical outcome (marked in purple), and Rho function pathway (marked in aqua) in expressed RhoAiso2-R176G LUAD patients.



(A)



(B)



(C)

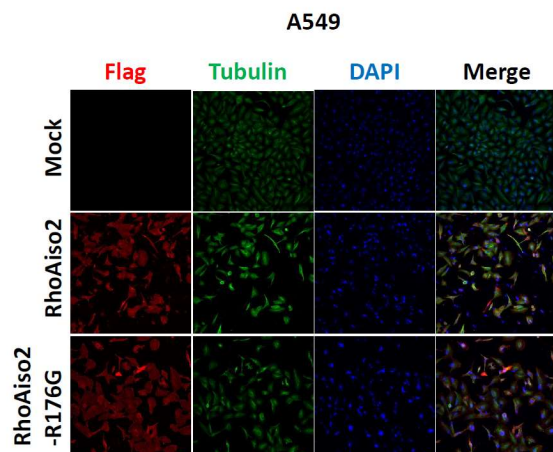


Figure 16 The protein expression level of RhoAiso2 and RhoAiso2-R176G in

LUAD cell lines

(A) RHOA isoform 2 (RHOAiso2) and the RHOAiso2-R176G variant constructs were cloned into pcDNA 3.0-Flag. (A-B) The expression intensity and efficiency were detected by western blot and immunofluorescence in LUAD cell lines CL1-5 and A549.



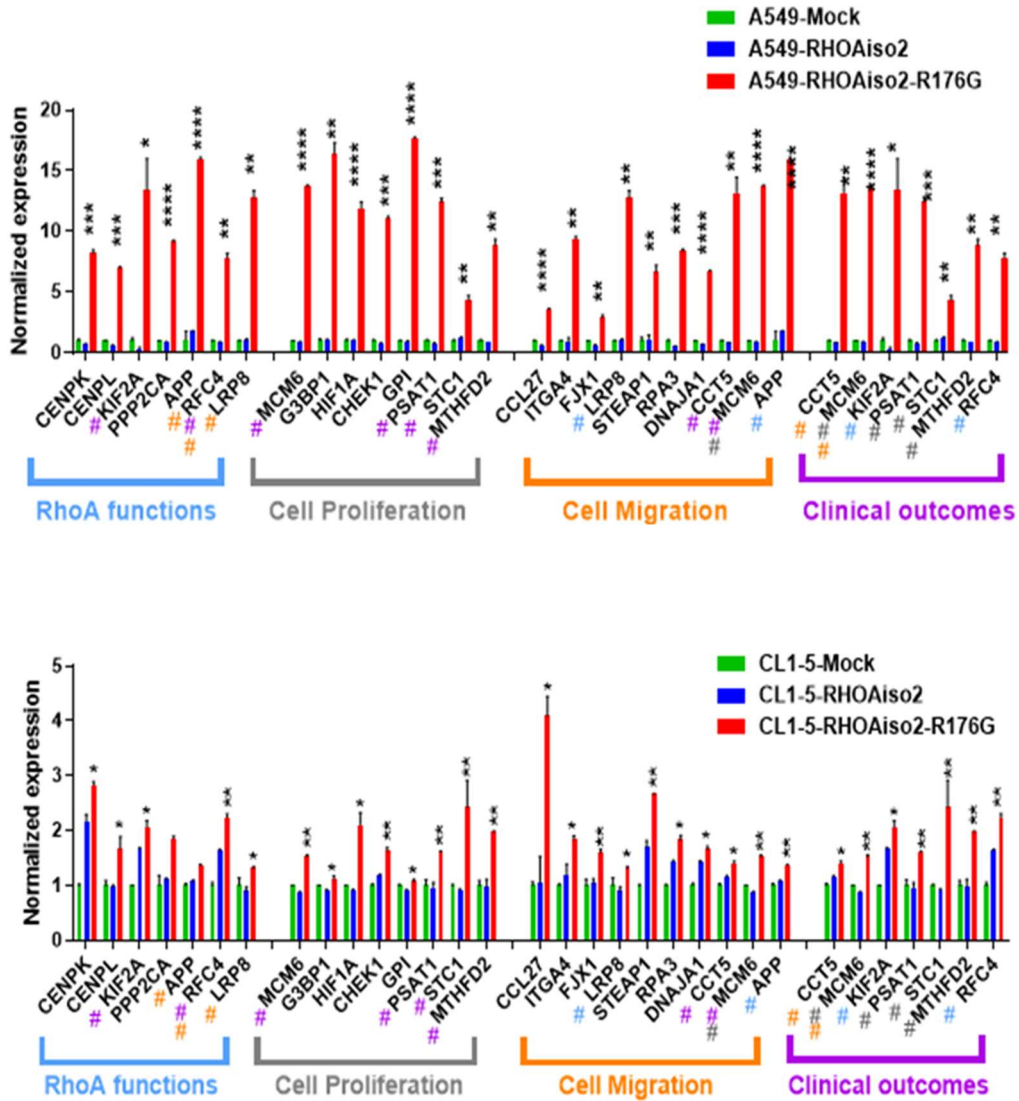
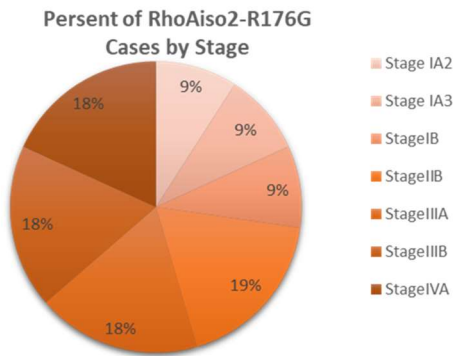


Figure 17 Validation of enrichment gene signatures in the RHOAiso2-R176G mutation compared with RHOAiso2- expressing LUAD cell lines.

Comparing the expression changes of the 22 genes in all four gene signatures by RT-

qPCR in CL1-5 and A549 cell lines which overexpressed RHOAiso2-R176G and RHOAiso2





Classification Table^a

Observed	Recurrence (0=X, 1=0)	Predicted		Percentage Correct
		0	1	
Step 1	Recurrence (0=X, 1=0)	0	34	.0
		1	81	100.0
Overall Percentage				70.4

a. The cut value is .500

Variables in the Equation

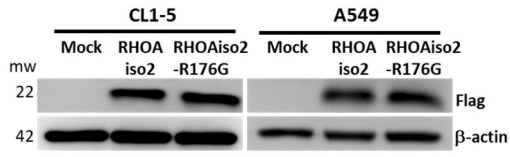
	B	S.E.	Wald	df	Sig.	Exp(B)
Step 1 ^a						
Gene(1)	.922	.450	4.202	1	.040	2.515
Constant	.208	.373	.309	1	.578	1.231

a. Variable(s) entered on step 1: Gene.

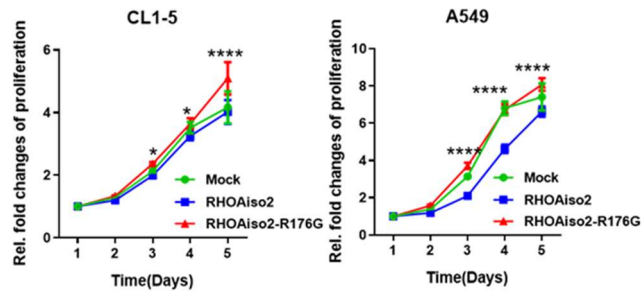
Figure 18 The distribution of present of RhoAiso2-R176G in 20 LUAD patients.



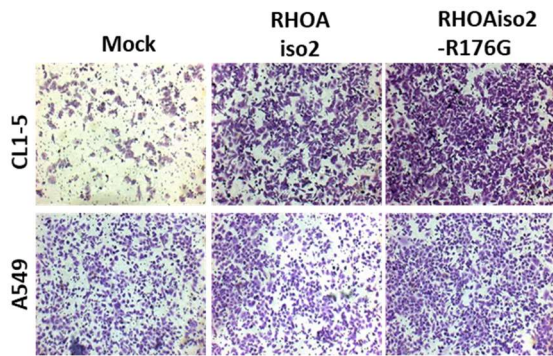
(A)



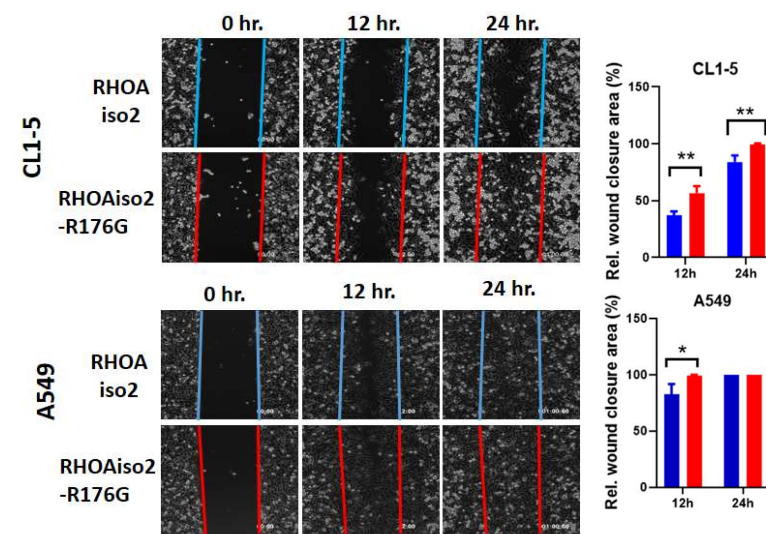
(B)



(C)



(D)



(E)

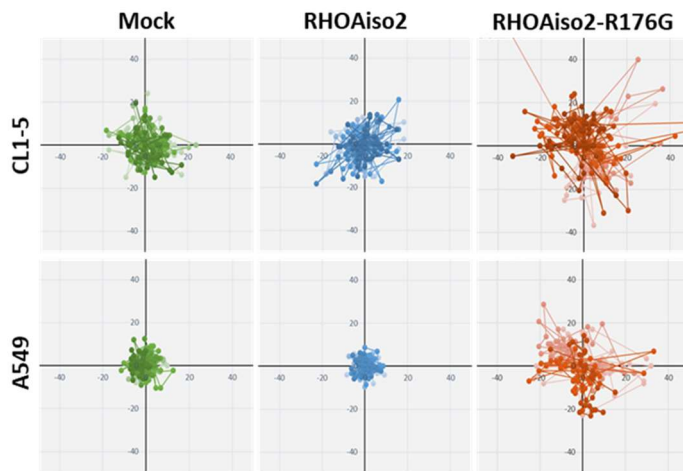


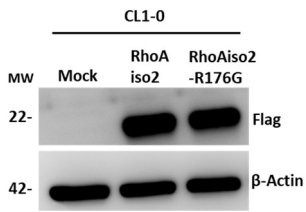
Figure 19 RHOAiso2-R176G promoted cell proliferation and migration in LUAD cell lines compared to RHOAiso2.

(A) The expression level of RHOAiso2 and RHOAiso2-R176G in cell lines were detected by western blot.

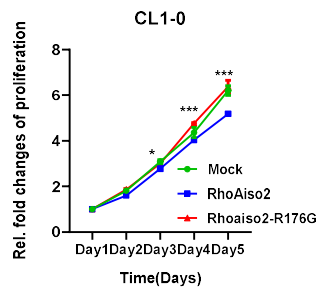
(B-E) Cell proliferation, wound healing, cell migration and cell tracking were detected in RHOAiso2 and RHOAiso2-R176G overexpressed CL1-5 and A549 cell lines.



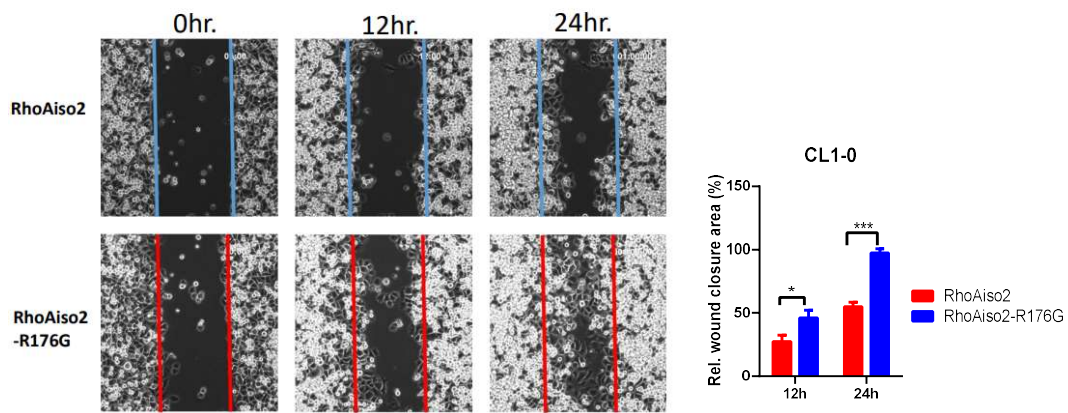
(A)



(B)



(C)



(D)

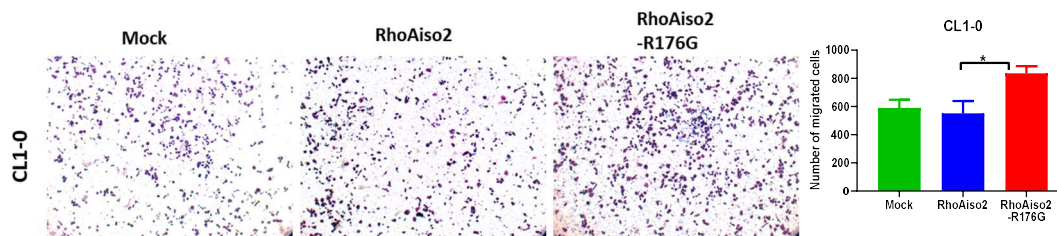


Figure 20 Expression of RHOAiso2-R176G mutation in LUAD cell line CL1-0

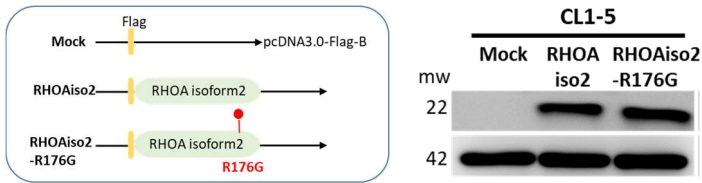
(A) Western blotting analysis.

(B) cell proliferation and cell migration with wound healing (C) and trans-well (D) assays.





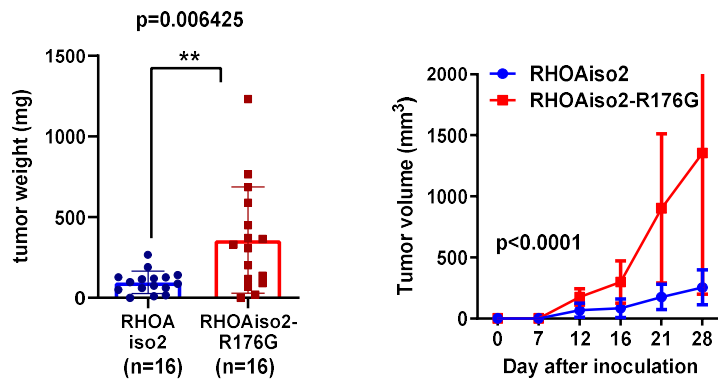
(A)



(B)



(C)



(D)

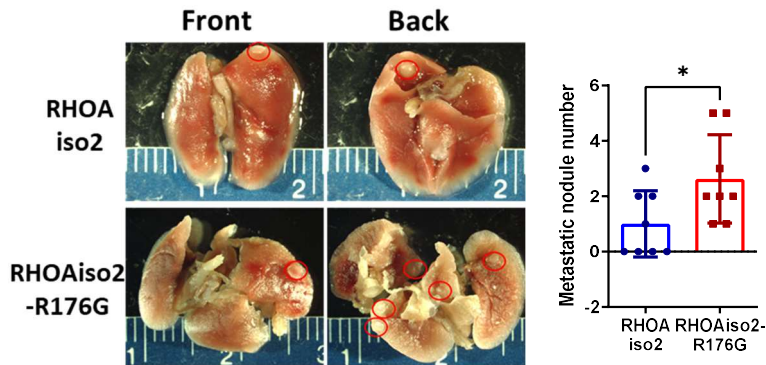




Figure 21 RHOAiso2-R176G variant promotes tumor growth and metastasis in vivo compared to RHOAiso2 .

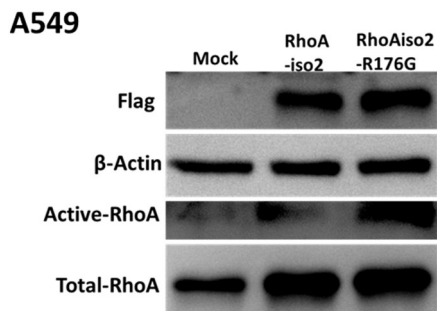
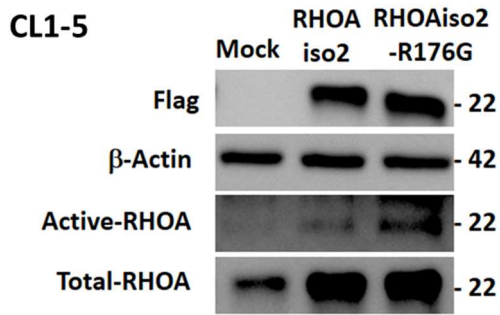
(A) The expression level of RHOAiso2 and RHOAiso2-R176G in cell lines were detected by western blot.

(B-C) The tumor weight and tumor volume were increased on the RHOAiso2-R176G variant compared to RHOAiso2 xenograft model.

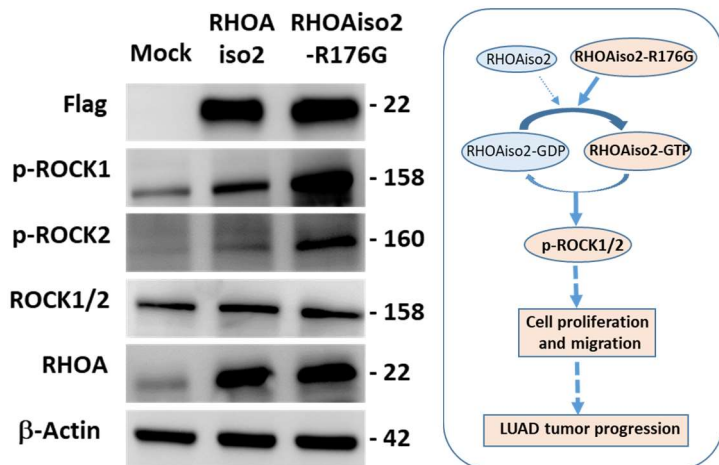
(D) The number of tumor nodules were increased in RHOAiso2-R176G variant metastasis mouse model which promoted tumor metastasis compared to RHOAiso2 mouse model by tail vein injection.



(A)



(B)





(C)

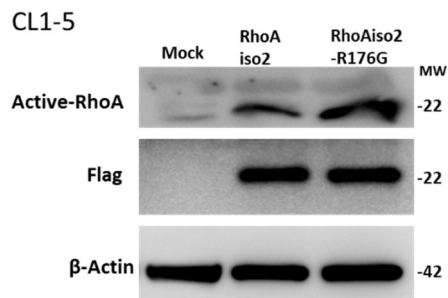


Figure 22 RHOAiso2-R176G specific variant increased RHOA-GTP activity and phosphorylated p-ROCK1/2 signaling.

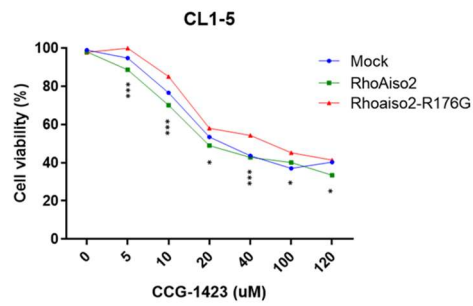
(A) RHOA activity were increased in RHOAiso2-R176G variant compared to RHOAiso2 by RHOA activity pull-down assay after RHOA activator was treated.

(B) The expression of phosphorylate Rock1/2 were enhanced in RHOAiso2-R176G variant compared to RHOAiso2.

(C) RHOA activity were increased in RHOAiso2-R176G variant compared to RHOAiso2 by RHOA activity pull-down assay after without RHOA activator treated.



(A)



(B)

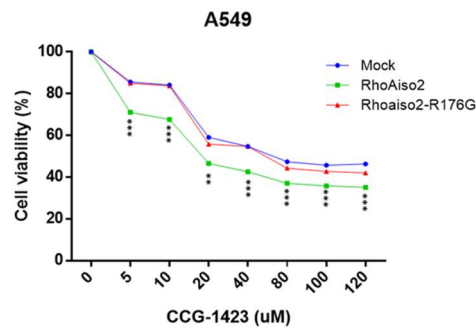


Figure 23 Expression of RhoAiso2-R176G increased cell viability at RhoA inhibitor CCG-1423 treated.

(A-B) Cell viability assay of expression of RhoAiso2R176G after treated CCG-1423 24

h.

Table 1 A-to-I editing events in 20 paired LUAD

Table 2 Statistics

Please refer to information available from <https://doi.org/10.1002/mc.23490>.



Primer sequences of selected RNA editing sites for SEQUENOM MassARRAY® System																										
WELL	TERM	SNP_ID	Primer_ID	2bp-PCR	1bp-PCR	AMP_LEN	UP_CONF	MP_CONF	Tm(NN)	PGC	PWARN	UEP_DIR	UEP_MASS	UEP_SEQ	EXT1_CALL	EXT1_MASS	EXT1_SEQ	EXT2_CALL	EXT2_MASS	EXT2_SEQ	EXT3_CALL	EXT3_MASS	EXT3_SEQ	EXT4_CALL	EXT4_MASS	EXT4_SEQ
W1	IPLEX	PPA_0109	70310	ACGTTGGAAACGTTGGAA	ACGTTGGAA	110	99.6	99.4	45	47.1		R	5123.4	CCTAAGCCG		5370.5	CCTAAGCCG		5450.5	CCTAAGCCCAATAGCT						
W1	IPLEX	MDM2_0109	70312	ACGTTGGAAACGTTGGAA	ACGTTGGAA	112	92.6	99.4	45.1	36.8 d		F	5875.9	AGGATAAAG		6147.1	AGGATAAAGTCTAGCTGAG		6163.1	AGGATAAAGTCTAGCTGAG						
W1	IPLEX	AZIN1	70471	ACGTTGGAAACGTTGGAA	ACGTTGGAA	92	99.7	98.4	46.6	52.9 d		F	5237.4	CTCAGGAAC		5484.6	CTCAGGAACAGACAGCT		5564.5	CTCAGGAACAGACAGCT						
W1	IPLEX	TUBGP2-DN	71828	ACGTTGGAAACGTTGGAA	ACGTTGGAA	94	97	93.5	51	66.7 d		R	4676.1	GGCGACAGG		4923.2	GGCGACAGGACAGAT		5003.2	GGCGACAGGACAGAT						
W1	IPLEX	RBMXL1-dD	71829	ACGTTGGAAACGTTGGAA	ACGTTGGAA	100	89	93.5	46.7	41.2		R	5173.4	TTGGTTTCAG		5420.6	TTGGTTTCAG		5500.5	TTGGTTTCAGGCTCTTT						
W1	IPLEX	RHOA-dNA	71830	ACGTTGGAAACGTTGGAA	ACGTTGGAA	100	92	93.5	47.9	52.9 g		F	5281.4	TGAGTAGCTA		5552.6	TGAGTAGCTA		5568.6	TGAGTAGCTGGGGTTACG						
W1	IPLEX	TUBGP2-gDN	71832	ACGTTGGAAACGTTGGAA	ACGTTGGAA	109	90.4	90.2	51	66.7 d		R	4676.1	GGCGACAGG		4923.2	GGCGACAGGACAGAT		5003.2	GGCGACAGGACAGAT						
W1	IPLEX	RBMXL1-gDI	71833	ACGTTGGAAACGTTGGAA	ACGTTGGAA	100	89	90.2	46.7	41.2		R	5173.4	TTGGTTTCAG		5420.6	TTGGTTTCAG		5500.5	TTGGTTTCAGGCTCTTT						
W1	IPLEX	RHOA-gDNA	71834	ACGTTGGAAACGTTGGAA	ACGTTGGAA	100	100	90.2	47.9	52.9 g		F	5281.4	TGAGTAGCTA		5552.6	TGAGTAGCTA		5568.6	TGAGTAGCTGGGGTTACG						



Table 3 Primer sequences of selected RNA editing sites for SEQUENOM

MassARRAY® System



Table 4 Primer sequences for RT-qPCR of selected genes in functions of RHOA

functions, cell proliferation, cell migration and clinical outcomes.



1	APP_F	TCTCGTTCCTGACAAGTGCAA
2	APP_R	GCAAGTTGGTACTCTTCTCACTG
3	CCL27_F	GCAGCATTCTACTGCCAC
4	CCL27_R	AGGTGAAGCACGAAAGCCTG
5	CCT5_F	TGGAAGTGTCCAAGTCTCAGG
6	CCT5_R	CATCGGCTATTCTGATTGGGTG
7	CENPK_F	AACACTCACCGATTCAAATGCT
8	CENPK_R	CAGTCAAGGGAATTGTTTCAGGT
9	CENPL_F	CACCAGAGTCAACTCCTAGTGC
10	CENPL_R	TCTGCTTCCTGACCGATTCTAA
11	CHEK1_F	CCAGATGCTCAGAGATTCTTCCA
12	CHEK1_R	TGTTCAACAAACGCTCACGATTA
13	DNAJA1_F	ACTGGAGCCAGGCGATATTAT
14	DNAJA1_R	CTTCAACGAGCTGTATGTCCAT
15	FJX1_F	CCGGCTCGTAAGCAACCTC
16	FJX1_R	AGCGGCTCGTTATACTTGTC
17	G3BP1_F	CGGGCGGGAATTTGTGAGA
18	G3BP1_R	TCTGTCCGTAGACTGCATCTG
19	GPI_F	CCGCGTCTGGTATGTCTCC
20	GPI_R	CCTGGGTAGTAAAGGTCTTGGA
21	HIF1A_F	ATCCATGTGACCATGAGGAAATG
22	HIF1A_R	TCGGCTAGTTAGGGTACACTTC
23	ITGA4_F	CACAACACGCTGTTCGGCTA
24	ITGA4_R	CGATCCTGCATCTGTAAATCGC
25	KIF2A_F	AAGGCAAAGAGATTGACCTGG
26	KIF2A_R	GAAGCTACAGTCCGTCGATTC
27	LRP8_F	CTGTGGCGACATTGATGAGTG
28	LRP8_R	TCTTGGTCAGTAGGTCCATCTC
29	MCM6_F	GAGGAACTGATTCGTCCTGAGA
30	MCM6_R	CAAGGCCCGACACAGGTAAG
31	MTHFD2_F	GATCCTGGTTGGCGAGAATCC
32	MTHFD2_R	TCTGGAAGAGGCAACTGAACA

33	PPP2CA_F	GTTCGTTACCGTGAACGCATC
34	PPP2CA_R	TGGCGAGAGACCACCATGT
35	PSAT1_F	TGCCGCACTCAGTGTTGTTAG
36	PSAT1_R	GCAATTCCCGCACACAAGATTCT
37	RFC4_F	TTGGGCCTGAACTTTTCCGAT
38	RFC4_R	AGCGACTTCCTGACACAGTTA
39	RPA3_F	AGCTCAATTCATCGACAAGCC
40	RPA3_R	TCTTCATCAAGGGGTTCCATCA
41	STC1_F	CACGAGCTGACTTCAACAGGA
42	STC1_R	GGATGTGCGTTTGATGTGGG
43	STEAP1_F	CCCTTCTACTGGGCACAATACA
44	STEAP1_R	GCATGGCAGGAATAGTATGCTTT
45	RhoaV3-F	AGGAGCCTCACTGTGTCGCCAGGCTGG
46	RhoaV3-R	TCAGGTTTCACCGGCTCCTGGGTGTG

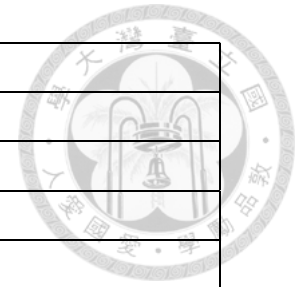


Table 5 Primer sequences for cloning and construction of RHOAiso2 and

RHOAiso2-R176G site mutagenesis.

1	RHOA- EcoRI F	F:AGCTGAATTCATGGCTGCCATCCGGAAG
2	RHOA- XhoI R	R:AGCTCTCGAGTCAGGTTTCACCGGCTC
3	SDM-RHOA- F	F:GTAGCTGGGGTTGCAGGCGCCCACTACCAC
4	SDM-RHOA- R	R:TGGGCGCCTGCAACCCCAGCTACTCAGGAG